A LABORATORY STUDY of the RELATION OF STRESS TO STRAIN for a CRUSHED LIMESTONE BASE MATERIAL

William M. Moore
Associate Research Engineer

Sylvester C. Britton
Associate Research Engineer

and

Frank H. Scrivner
Research Engineer

Research Report Number 99-5F
Stress Distribution in Granular Masses
Research Study Number 2-8-65-99

Sponsored by

The Texas Highway Department
In Cooperation with the
U. S. Department of Transportation
Federal Highway Administration

September, 1970

TEXAS TRANSPORTATION INSTITUTE
Texas A&M University
College Station, Texas

Preface

This is the fifth and final report issued under Research Study 2-8-65-99, Stress Distribution in Granular Masses, which was conducted at the Texas Transportation Institute as part of the cooperative research program with the Texas Highway Department and the Department of Transportation, Federal Highway Administration.

The first four reports are:

"The Use of Particulate Mechanics in the Simulation of Stress-Strain Characteristics of Granular Materials," by James C. Armstrong and Wayne A. Dunlap, Research Report 99-1, Texas Transportation Institute, August, 1966.

"A Gyratory Compactor for Molding Large Diameter Triaxial Specimens of Granular Materials," by Lionel J. Milberger and Wayne A. Dunlap, Research Report 99-2, Texas Transportation Institute, October, 1966.

"Evaluation of the TTI Gyratory Compactor," by William M. Moore and Lionel J. Milberger, Research Report 99-3, Texas Transportation Institute, February, 1968.

"Deformation Measuring System for Repetitively Loaded, Large Diameter Specimens of Granular Material," by William M. Moore, Gilbert Swift, and Lionel J. Milberger, Research Report 99-4, Texas Transportation Institute, August, 1969.

The authors wish to thank all members of the Institute who assisted in this research. They would like to express special appreciation to Mr. Ronnie Surovik for his assistance in the development of data reduction techniques, Mr. C. H. Michalak for his assistance in data reduction and report preparation, and Mr. Gene Schlieker for his assistance in all phases of the research.

Thanks are also expressed to Mr. Kelsey Martin of Martin Research Associates for his initial concepts of the optical tracker used in this research and his advice and assistance in developing operational techniques to adapt the instrument to our research problem.

The authors also wish to thank Mr. James L. Brown, the Texas Highway Department Study Contact Representative, for his assistance and support in this research.

The opinions, findings, and conclusions expressed in this publication are those of the authors and not necessarily those of the Department of Transportation, Federal Highway Administration.

Abstract

A newly developed optical tracker measuring system was used for observing the dynamic displacement vector at points on the periphery of a compacted triaxial test specimen of granular material subjected to rapid, repetitive loading. The material was a crushed limestone of the type used in highway pavements.

The displacement data were converted to components of normal strain, and a mathematical model was developed that expressed each strain component as a function of the applied stresses. The model contained a variable modulus dependent upon both the lateral pressure applied to the specimen and its stress history.

Summary

The research reported herein was aimed at helping to establish some basic relationship between stress and strain within a mass of granular material. To this end, a newly developed optical tracker was employed for observing the dynamic displacement vector at points on the periphery of a cylindrical triaxial test specimen of crushed limestone subjected to rapid loading.

Except for brief, infrequent intervals devoted to the acquisition of displacement data for selected combinations of lateral and vertical loadings, the 6-inch diameter by 8-inch high specimen was subjected to a constant lateral pressure of 20 psi, and a repetitive deviator pressure of 34 psi. The latter was applied and released within 0.2 second, and was repeated every two seconds. A total of 2.5 million vertical load applications was made on the specimen during the testing program.

The displacement data taken at points in the central region of the specimen - where the stresses were assumed to be reasonably uniform at any given instant - were converted to axial and circumferential strain components. The strain components were analyzed with respect to their relationship to the applied pressures. The following principal conclusions were drawn:

(1) Throughout a rapid increase in the deviator stress, the lateral pressure meanwhile being held constant, the vertical strain at any instant was directly proportional to the deviator stress at that instant, and inversely proportional to the square of the lateral pressure plus a constant. That is,

$$\text{Vertical strain} = \frac{\text{Constant x Deviator stress}}{\text{Constant + (Lateral stress)}}^2$$

The two constants in the equation were different.

(2) Similarly, it was found that

$$\text{Circumferential strain} = -\frac{\text{Constant x Deviator stress}}{\text{Constant + (Lateral stress)}}^2$$

where the constants were different from each other and from the constants in the equation for vertical strain.

(3) The stiffness of the material in the radial direction differed from its stiffness in the vertical direction; that is, the specimen was anisotropic.

(4) The stiffness in both directions (radial and vertical) increased markedly as the number of load applications increased.

(5) Although the tests were performed at two widely different loading rates, the effect of loading rate was small and inconsistent.

(6) In a special test on a different but nearly identical specimen it was found that the resilient modulus of the specimen tended to gradually--rather than instantaneously--decrease when the lateral pressure was set at a value less than that used in conditioning the specimen.

In general it was concluded that it may not be possible, even in a controlled environment, to predict with precision how a laboratory specimen of granular material will behave when loaded at a given point in time, unless its behavior at some past instant has been determined, and its entire stress history from that time to the present is known. It follows that accurate predictions, on a routine basis, of traffic induced stresses and strains in a flexible pavement are not within our grasp, at least for the present.

Implementation Statement

When combined with information on elastic modulii being gathered in Studies 123 and 136, the results of Study 99 are expected to be used in documenting the introduction of the theory of elastic layered systems into the Flexible Pavement Design System now on trial in the Texas Highway Department.

Table of Contents

List of Figures

List of Tables

1. Introduction

A truly rational system for the design of flexible pavements must include realistic physical equations - or computer oriented procedures - from which traffic-induced stresses and deformations can be estimated. The first step in the derivation of such equations or procedures is to find, from laboratory and in situ testing, a set of basic relationships (sometimes referred to as "constitutive equations," and sometimes as "a deformation hypothesis") from which one can predict, with acceptable accuracy, the deformations of flexible pavement materials when subjected to any given state of stress. Study 2-8-65-99, and its predecessor, Study 2-8-62-27, were devoted to a search for these basic relationships within the laboratory.

The prime purpose of Study 99 was to test the validity of the deformation hypothesis for granular materials developed in Study 27, and, if necessary, to revise it. This report contains the results of the testing and analysis work directed toward accomplishing this goal.

The hypothesis developed in Study 27 was originally proposed by Dunlap (1) and was later extended by Scrivner (2). In the extended form it consists of a set of three simultaneous equations, relating normal strain to normal stress, which are analogues of the well-known Hooke's Law equations of elasticity theory. These equations were based upon estimates of axial strain occurring during the triaxial testing of a large number of granular materials. Axial strain estimates were computed from measurements of the vertical displacement of the triaxial loading rod, which was assumed to be equal to the shortening of the specimen under load. Several attempts (3) made in Study 27 to measure the radial expansion of the specimen to provide data for testing Scrivner's hypothesis were not very conclusive. Later, in the present study, the assumption that the loading rod motion was equivalent to the total shortening of the specimen was found to be incorrect (4).

Early in the analysis phase of the present study it became apparent that the deformation hypothesis proposed in Study 27 was not suitable for predicting the lateral displacements observed. After improvement of the measurement system, it was a simple matter to test the hypothesis; to evaluate the validity of the set of equations required only accurate values of all the variables. However, after the hypothesis was rejected there remained an infinite number of possibilities to be investigated.

During the analysis phase the authors have tried many possible models to represent the observed behavior. Although a model has been found that fits the data quite well, the authors realize that a better one may be devised.

The stress-strain data used in the analysis are believed to be the most accurate that have been taken to date on a specimen of granular material. Since these data can be used to test other hypotheses, they have been included in the appendix. For a complete description of the test equipment, method of measurement, and technique of data reduction, the reader is referred to Research Report 99-4 (4).

2. Background

Based on measured values of load, loading rod motion and triaxial confining pressure, Dunlap advanced the following equation for axial strain, which fitted the data from either repetitive or slow speed tests (1):

$$\varepsilon_z = \frac{\sigma_z - k_1 (\sigma_r + \sigma_\theta)}{k_2 + k_3 (\sigma_r + \sigma_\theta)} \tag{1}$$

where σ_z, σ_r, σ_θ are the normal stresses in cylindrical coordinates, and

ε_z, ε_r, ε_θ are the normal strains in cylindrical coordinates.

(Compressive stresses and strains are regarded as positive).

In the development and testing of this hypothesis Dunlap made the following commonly used assumptions:

$$\sigma_z = P/A + \sigma_c$$

$$\sigma_r = \sigma_\theta = \sigma_c$$

$$\varepsilon_z = \Delta/H$$

where P = force applied to loading rod,

A = cross-sectional area of test specimen,

σ_c = triaxial confining pressure,

Δ = displacement of loading rod, and

H = height of test specimen.

After considering the form of the equation, Scrivner proposed the following extension (2):

$$\varepsilon_z = \frac{\sigma_z - k_1 (\sigma_r + \sigma_\theta)}{k_2 + k_3 (\sigma_r + \sigma_\theta)} \tag{1}$$

$$\varepsilon_\theta = \frac{\sigma_\theta - k_1 (\sigma_z + \sigma_r)}{k_2 + k_3 (\sigma_z + \sigma_r)} \tag{2}$$

$$\varepsilon_r = \frac{\sigma_r - k_1 (\sigma_\theta + \sigma_z)}{k_2 + k_3 (\sigma_\theta + \sigma_z)} \tag{3}$$

Since the additional two equations were not based upon measured data, several attempts (3) were made in Study 27 to obtain estimates of circumferential strain; however, none were suitable for determining the validity of Scrivner's extension without ambiguity. Study 99 was initiated with the primary purpose of obtaining such data.

As the first step in acquiring the data, a special gyratory compactor, capable of producing more uniform specimens, was developed (5, 6), as well as an optical displacement measurement system which could be used to estimate both the axial and the circumferential strain on the periphery of a dynamically loaded triaxial test specimen (4). The first data obtained with this measurement system indicated that the strain calculated by dividing loading rod displacement by specimen height (the commonly used assumption for estimating ε_z) was always larger than the true value of ε_z. However, the rod motion did appear to be proportional to the axial strain so the significance of this finding was not clear. If the proportionality constant was independent of the confining pressure it might simply mean that the values of k_2 and k_3 estimated by Dunlap were somewhat smaller than their true values.

The assumptions used in the analysis reported here are as follows:

$\sigma_z = P/A + \sigma_c$

$\sigma_r = \sigma_\theta = \sigma_c$

ε_z = vertical strain in the <u>central portion</u> of the test specimen's periphery, estimated from vertical displacement data

ε_θ = circumferential strain in the <u>central portion</u> of the test specimen's periphery, estimated from horizontal displacement data

It was assumed that the stress-strain state in the central portion of a test specimen is uniform.

3. Testing Program

Basically the constitutive equations for granular flexible base materials should relate to the in situ gradation, moisture contents, and densities that exist during the life of a pavement structure. Thus, it was originally planned to test several materials at several levels of moisture content and density. However, due to time and manpower limitations, this was impossible. To characterize the vertical and radial strain for a single test as described in Report 99-4 required about 2000 hand measurements from four traces on 36 chart records (4). These data were punched on IBM computer cards and reduced using standard data processing techniques. Although considerable data processing was done by computer, the total data reduction for a single test required about three man-weeks. This time and manpower requirement probably could have been vastly reduced had analog to digital data acquisition equipment been available.

The experiment design for the analysis presented in the next section consists of 24 tests made on a single carefully prepared specimen as indicated below:

Variable	No. Levels	Levels
Confining pressure	3	10, 20, 30 psi
Loading rate	2	Slow (200 psi/sec, nominal) Fast (650 psi/sec, nominal)
Load applications	4	0.05, 0.25, 0.75, 2.5 millions

Total number of tests = 3 x 2 x 4 = 24

It was thought that the experiment described above would provide adequate data to test the deformation hypothesis and also that it would lead to a technique that could be used in subsequent experiments designed to characterize other significant variables. Some of the reasons for the selection of the variables included in the above experiment are given below.

Confining pressure - Several levels of this variable are required to vary the parameters in Scrivner's equations.

Loading rate - This variable was thought to be highly significant.

Number of load applications - Initially the relative significance of this variable was not clear; however, during the pilot testing it was learned that it was the most significant of the variables affecting the behavior of a test specimen. Since in highways the number of load applications is ever increasing, this variable is considered to be one of primary importance.

The test specimen was prepared using the material and compaction procedure described in Research Report 99-3 (5). The material, a high quality crushed limestone widely used in Texas, was compacted in the TTI Gyratory Compactor developed by Milberger and Dunlap (6). The compactor variables were selected in order to produce relatively high levels of moisture content and dry density (5.5 per cent and 141 pcf, respectively which corresponds to 2.3% air voids).

Following compaction, the specimen - protected by a rubber membrane to which optical targets had been attached (Figure 1) - was placed in the loading apparatus and the testing program was initiated.

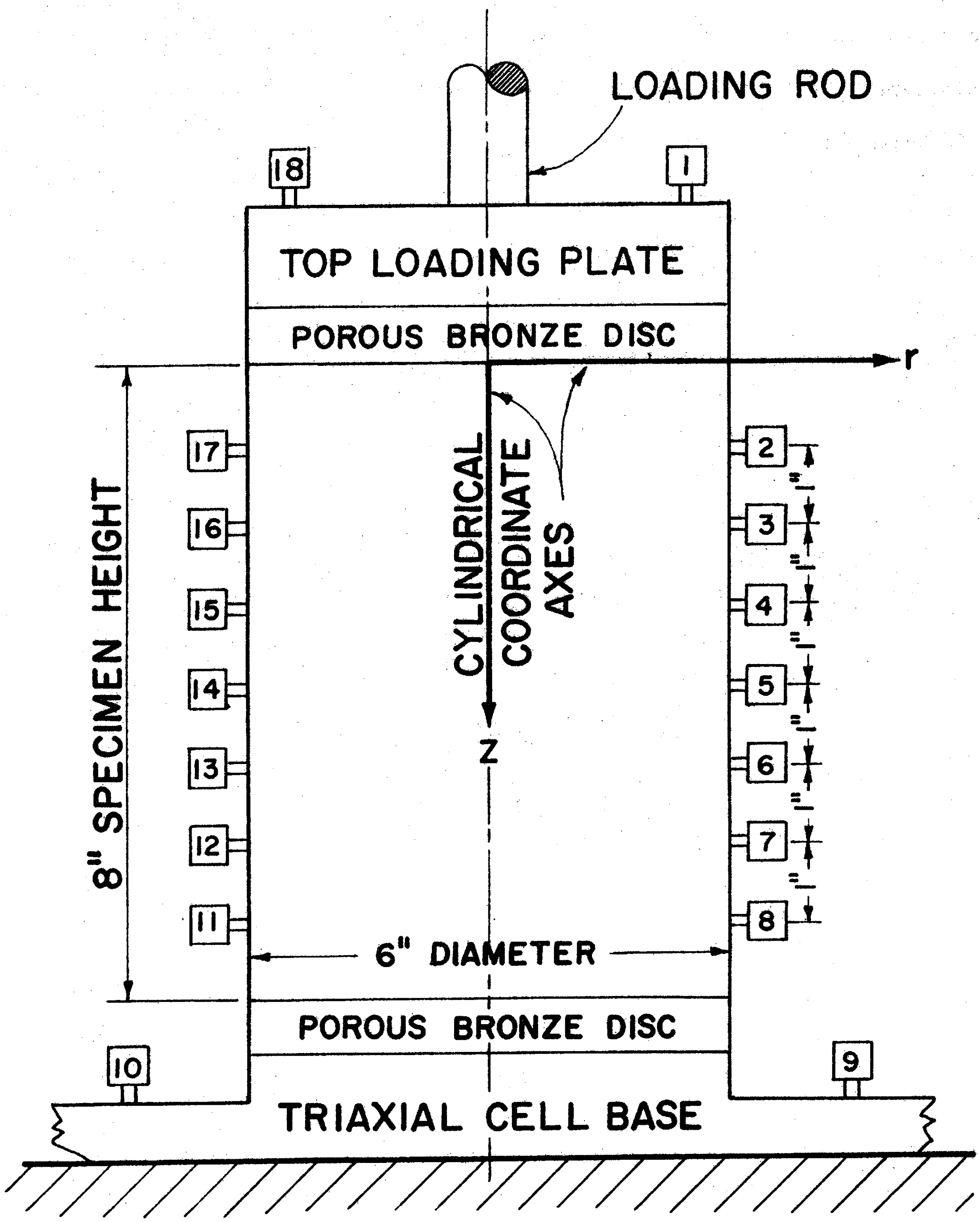

FIGURE 1 - Schematic of test specimen with optical targets attached.

The testing schedule followed in performing the experiment set forth above is given in Table 1. This experiment is referred to herein as the "main experiment" to distinguish it from the "special experiment" described in Section 4.6.

Table 1: Testing Schedule,
Main Experiment

Load Appl. (millions) * From-To	Increment	Beginning Date	Lateral Press. (psi)	Loading Rate	Test No.
0-0.045	0.045	7-22-69	20	Fast	None
0.045-0.053	0.008	7-23-69	10,20,30	Fast	1,2,3
0.053-0.062	0.009	7-24-69	20	Slow	None
0.062-0.067	0.005	7-24-69	10,20,30	Slow	4,5,6
0.067-0.242	0.175	7-25-69	20	Slow	None
0.242-0.244	0.002	7-29-69	20	Fast	None
0.244-0.247	0.003	7-29-69	30,20,10	Fast	7,8,9
0.247-0.287	0.040	7-30-69	20	Slow	None
0.287-0.292	0.005	7-31-69	30,20,10	Slow	10,11,12
0.292-0.729	0.437	7-31-69	20	Fast	None
0.729-0.733	0.004	8-11-69	10,20,30	Fast	13,14,15
0.733-0.809	0.076	8-12-69	20	Slow	None
0.809-0.815	0.006	8-13-69	10,20,30	Slow	16,17,18
0.815-2.390	1.575	8-13-69	20	Slow	None
2.390-2.482	0.092	9-22-69	20	Fast	None
2.482-2.488	0.006	9-24-69	30,20,10	Fast	19,20,21
2.488-2.503	0.015	9-24-69	20	Slow	None
2.503-2.505	0.002	9-25-69	30,20,10	Slow	22,23,24

* Deviator Stress of 34 psi applied every two seconds. Load applied and released in 0.2 second.

4. Analysis

4.1 Initial Data Reduction: Data from a typical test in the current experiment are displayed in Figure 2 and similar data obtained on a plastic cylinder are shown for comparison in Figure 3. The data plotted in Figure 2 were taken from Table A-17 in Appendix A and those in Figure 3 from Research Report 99-4 (4); Figure 3 is a replica of Figure 14 from that report. The abscissa, z, represents the vertical distance measured down from the top of an 8 inch high specimen. The ordinates, w and u, represent the vertical and radial displacement, respectively, of a point on the periphery of the specimen, while the numbers shown on the curves represent the vertical force applied to the loading rod of the triaxial apparatus. Thus, each plotted point on the upper graph represents the vertical displacement of a point on the periphery of the specimen at depth z, at the instant the applied load reached the value indicated on its curve, and the lower graph represents similar plots of radial displacement data.

One can note that typical data taken on the crushed limestone in the current experiment (Figure 2) are more erratic than those taken on the plastic (Figure 3). This, of course, is due in large part to the non-homogeneity of the crushed limestone.

As mentioned previously (Section 2), conventional assumptions were used to obtain stress data for analysis. That is, the lateral confining pressure was assumed to be equal to both σ_r and σ_θ, and the force applied to the loading rod of the triaxial apparatus, divided by

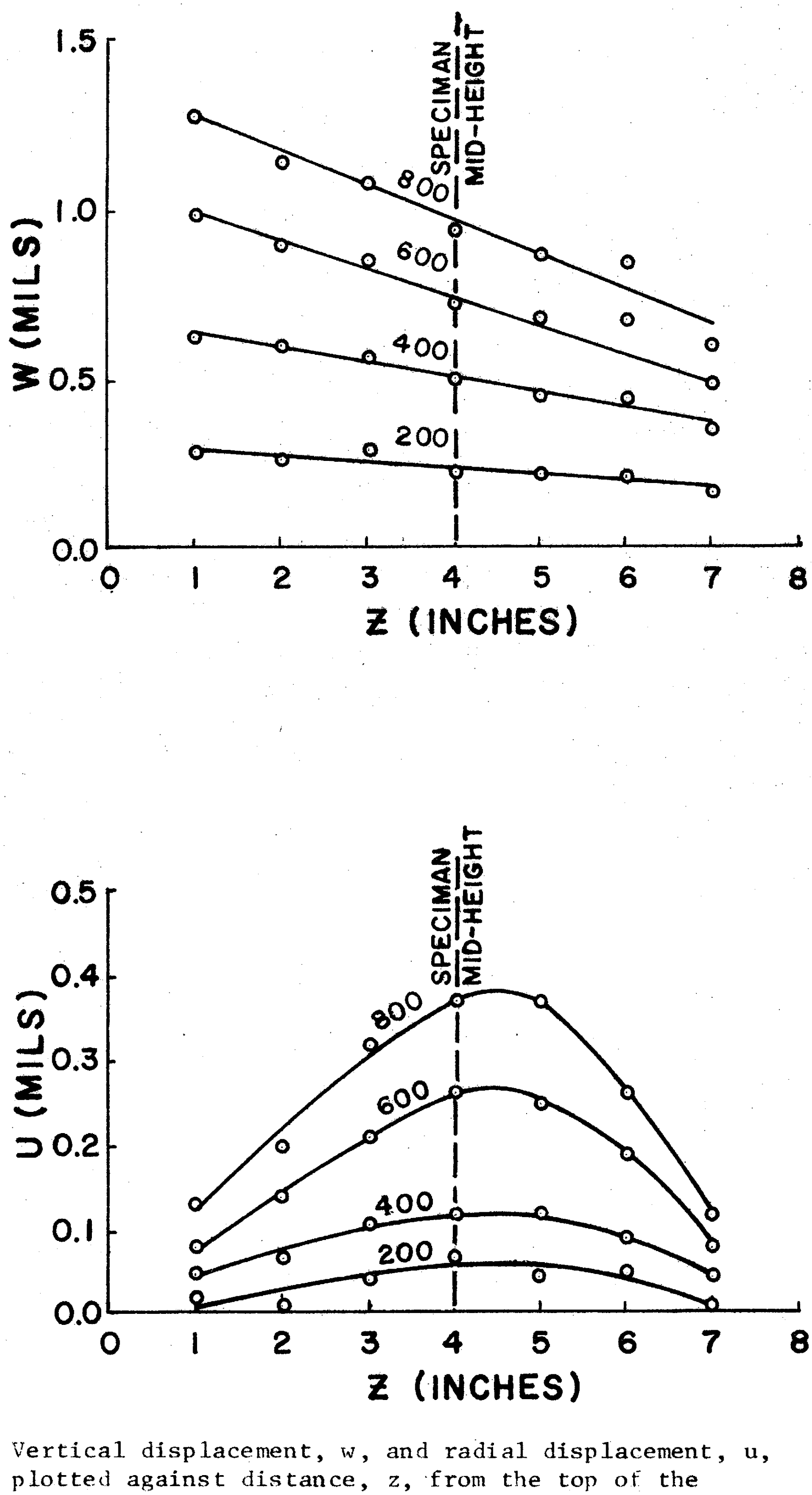

FIGURE 2 - Vertical displacement, w, and radial displacement, u, plotted against distance, z, from the top of the specimen. These data are from a typical test of the series reported herein. The numbers of the curves refer to vertical force on loading rod.

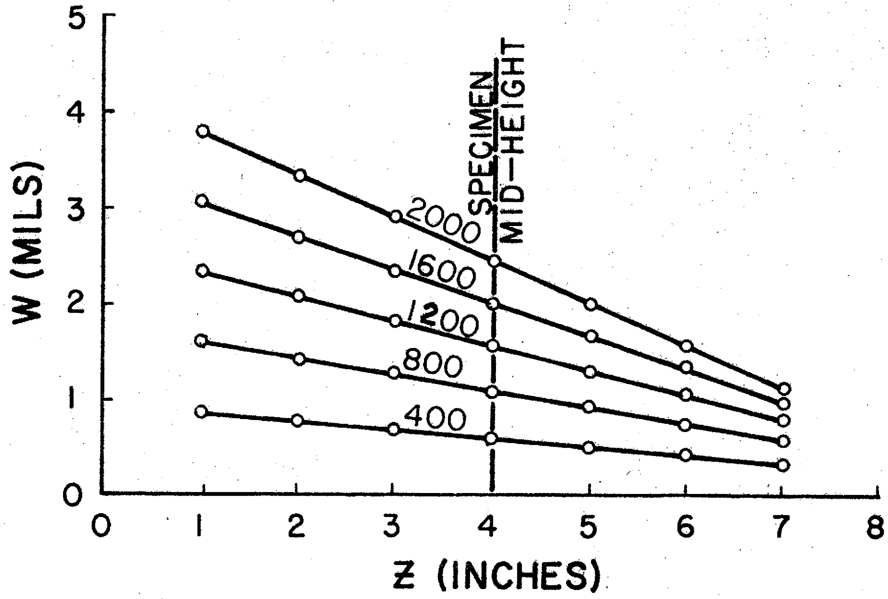

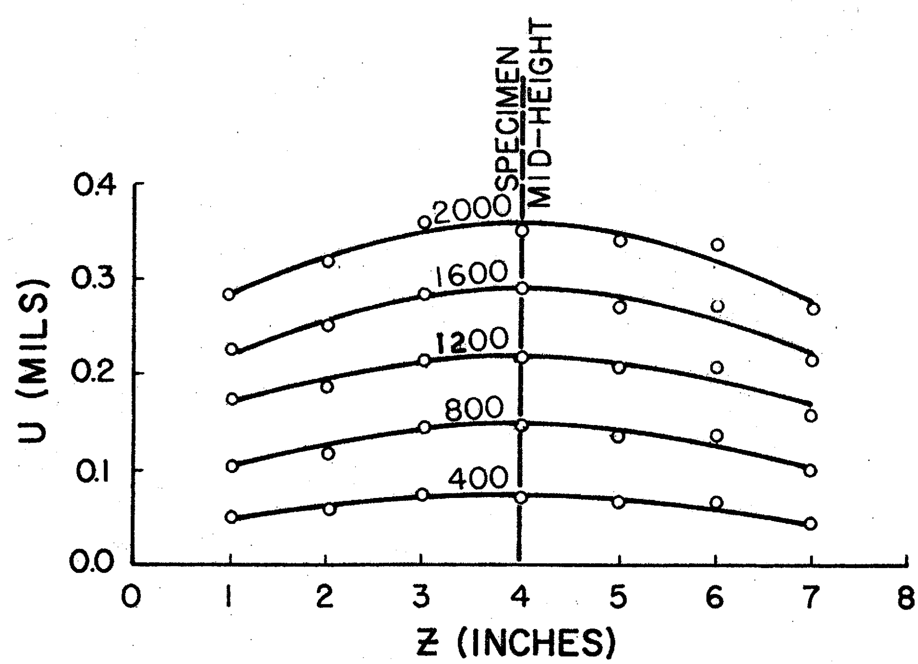

FIGURE 3 - Vertical displacement, w, and radial displacement, u, plotted against distance, z, from the top of the specimen. Data taken on a Lexan plastic cylinder. The numbers on the curves refer to the vertical force on loading rod.

the original cross-sectional area of the specimen, was assumed to represent the deviator stress, $\sigma_z - \sigma_r$. However, a completely new approach was used to estimate strains. Values of ε_z were taken to be slopes of linear regression lines fitted to the w versus z data given in Appendix A. For each of the twenty-four tests, values of ε_z were obtained for eight different values of applied load. The correlation coefficients for these 192 linear regressions ranged from 0.702 to 0.995 and averaged 0.953. Values for ε_θ were obtained by averaging the three central values of u, (i.e. the values at z = 3, 4 and 5) and dividing this average by the radius of the specimen. Tabular values of all stress-strain data are given in Appendix B.

4.2 Plots of Stress-Strain Data: To provide a "first look" at the stress-strain data recorded in Appendix B, the vertical stress, σ_z, was plotted against the vertical strain, ε_z, and against the circumferential strain, ε_θ, as shown in Figures 4 through 7. In the caption of each figure is given the average value of accumulated load applications, N, associated with the data plotted on that figure. In all cases the number of load applications expended in acquiring the data displayed on one of these figures is small compared to the number occurring between successive figures; thus, when comparing one figure with another, one may regard the variable, N, as fixed at the value shown on each figure.

An examination of Figures 4 through 7 led to the following conclusions:

(1) The data points associated with a constant lateral pressure, σ_r, and a fixed value of N, tended to scatter about a

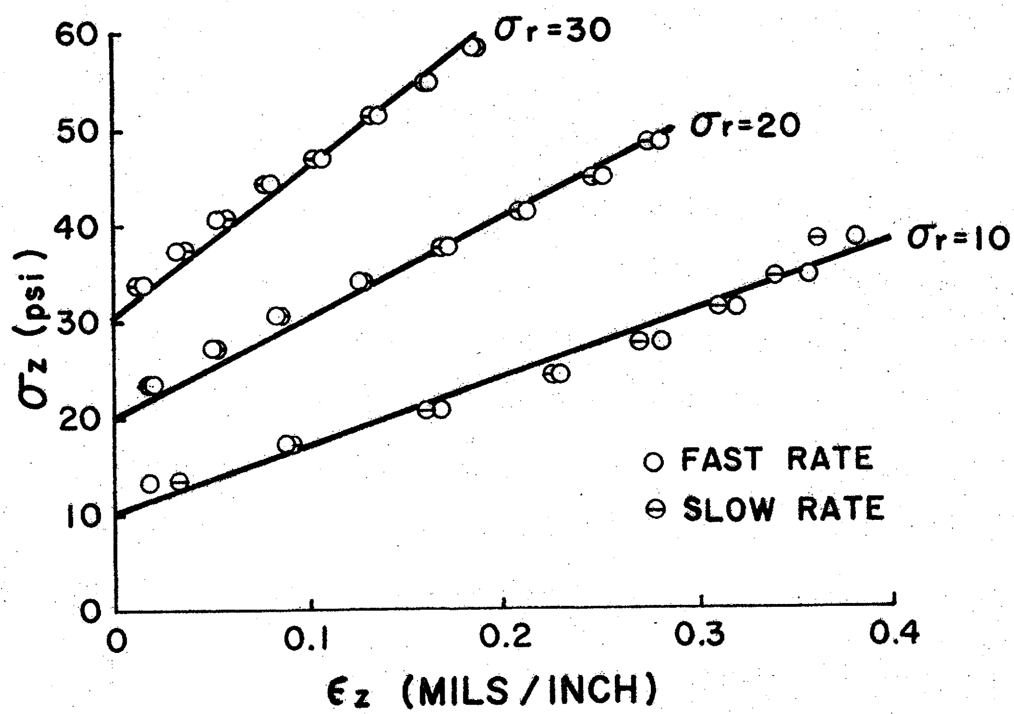

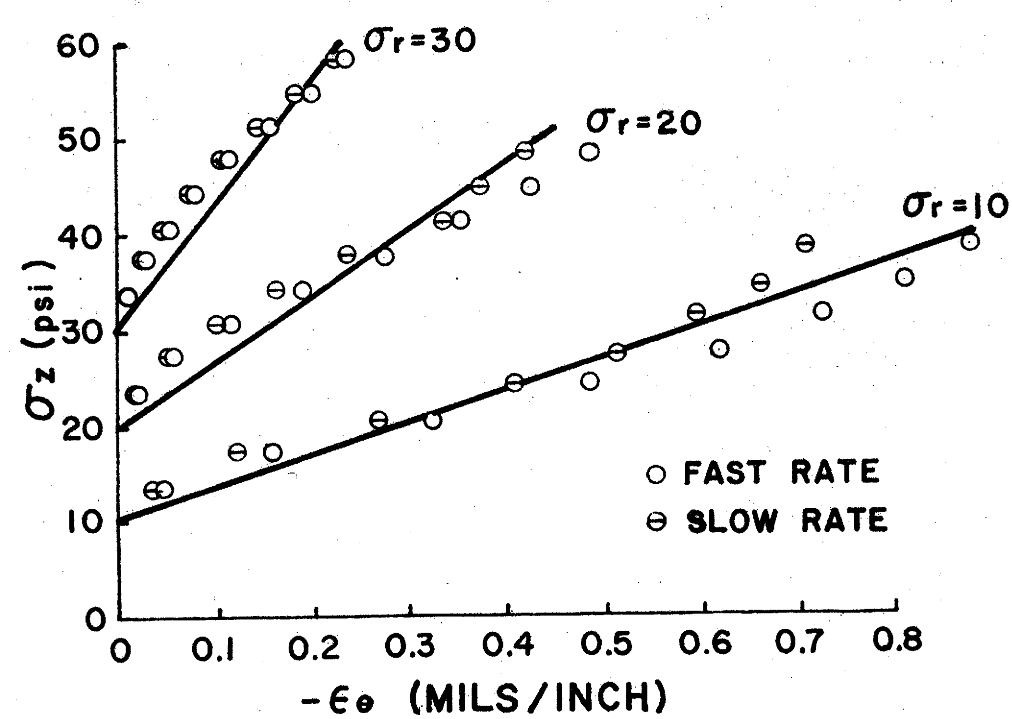

FIGURE 4 - Stress-strain data from Tests 1 through 6, taken at N = 0.06 million.

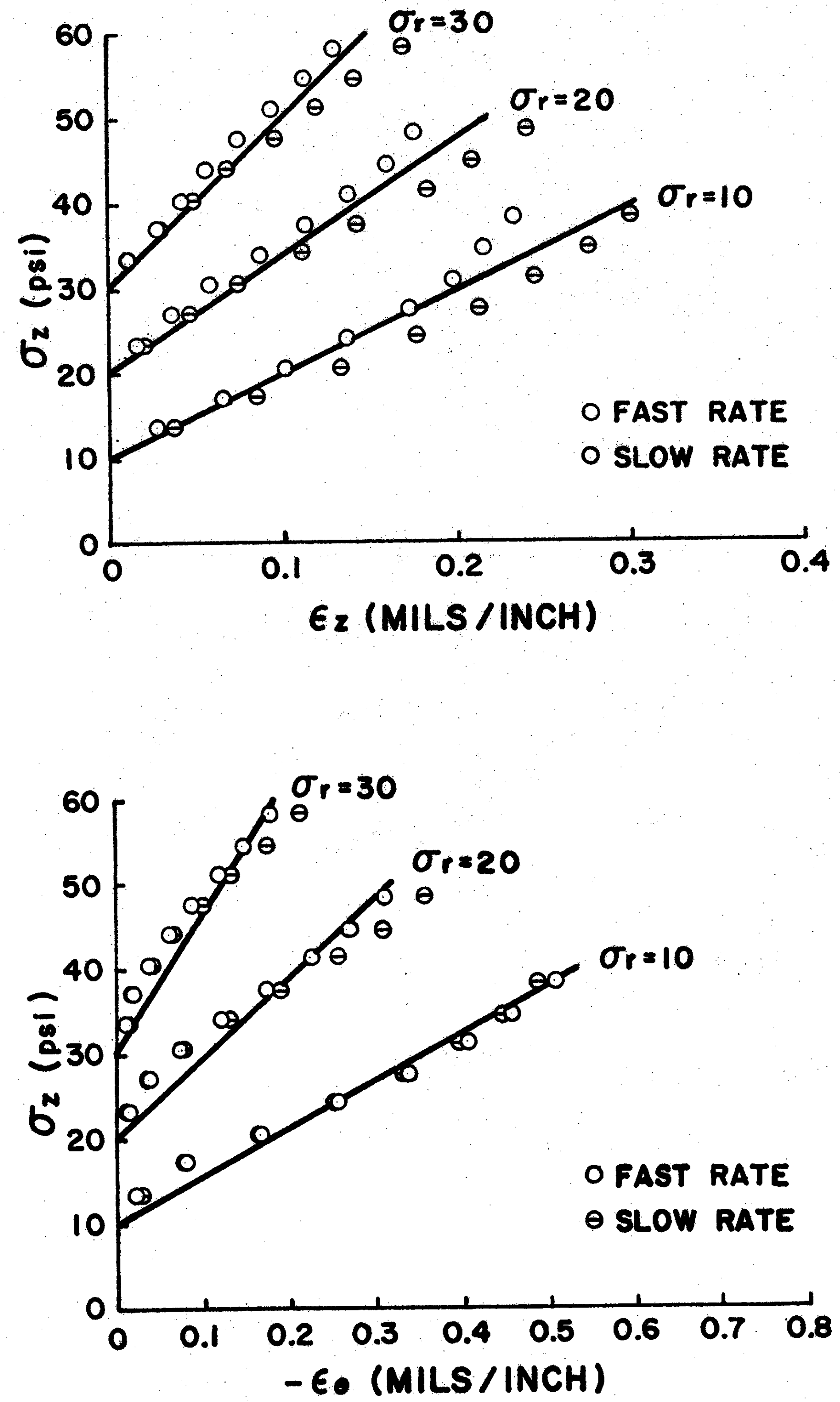

FIGURE 5 - Stress-strain data from Tests 7 through 12, taken at N = 0.27 million.

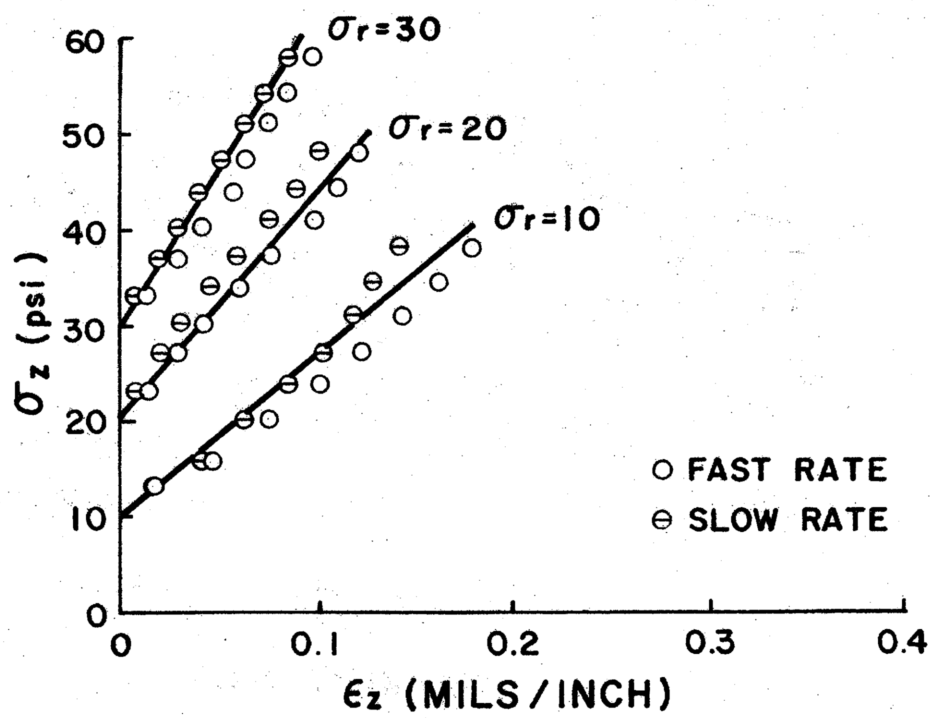

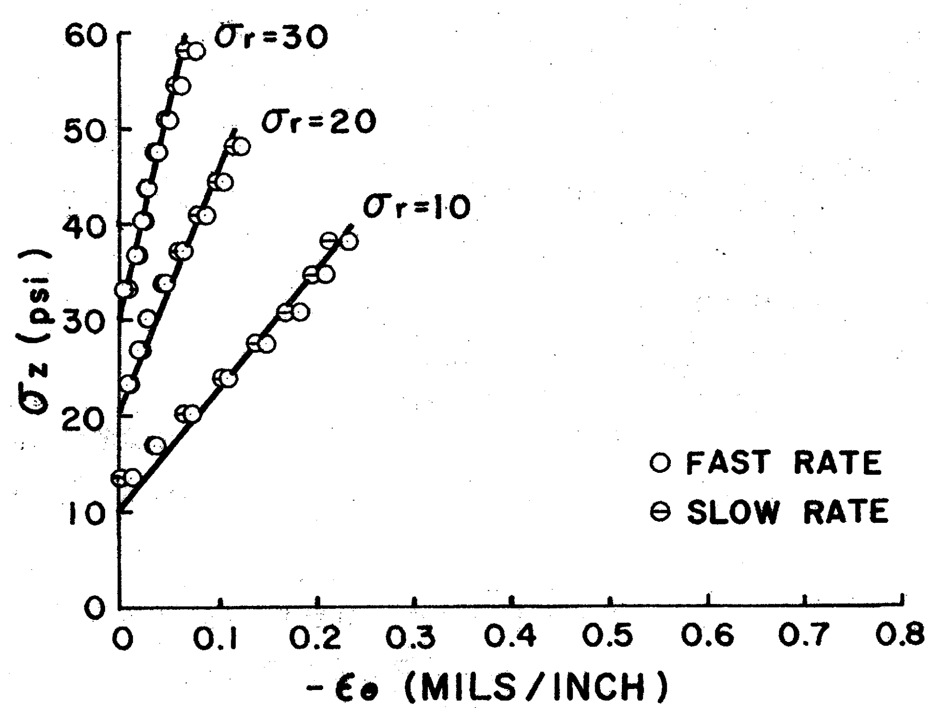

FIGURE 6 - Stress-strain data from Tests 13 through 18, taken at N = 0.77 million.

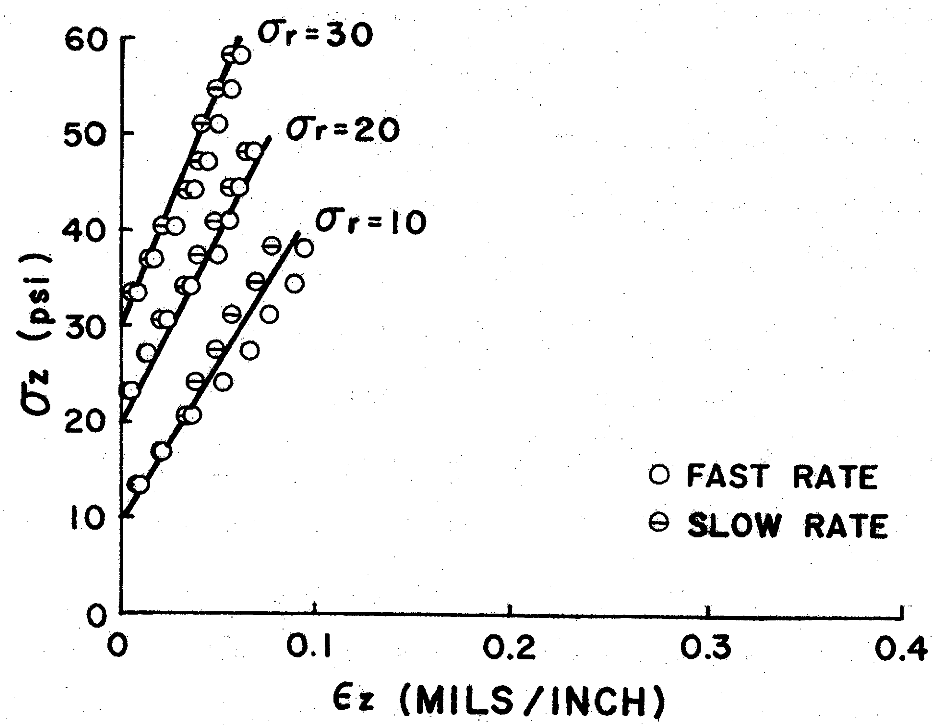

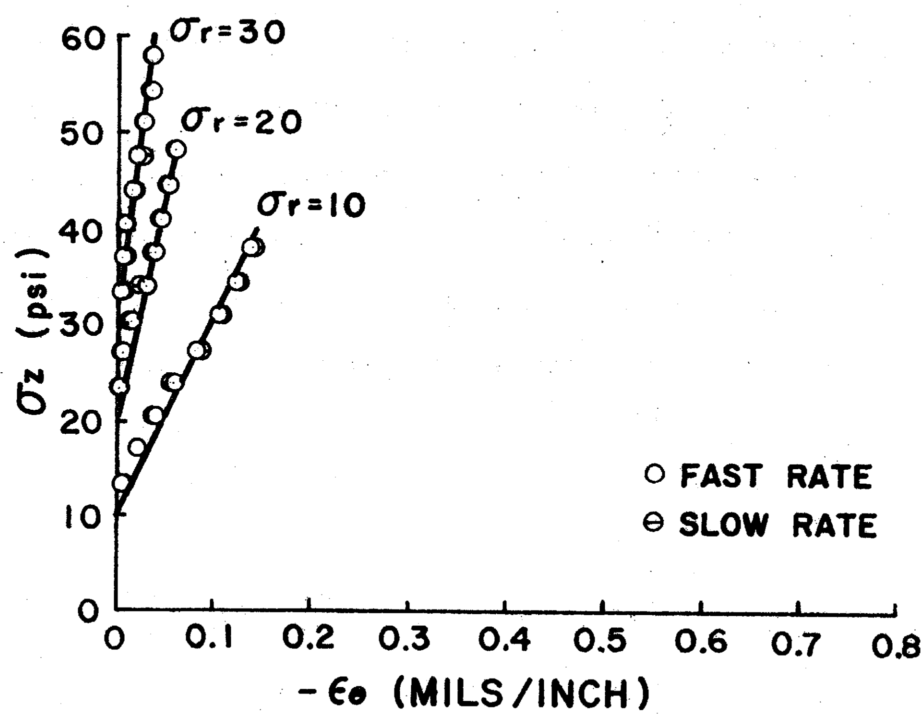

FIGURE 7 - Stress-strain data from Tests 19 through 24, taken at N = 2.49 millions.

straight line, although some minor curvature - particularly at low values of strain - was apparent.

(2) For a fixed value of N, the slope of straight lines drawn through the data tended to increase as σ_r increased.

(3) For a fixed value of σ_r, the slope of straight lines drawn through the data tended to increase as N increased.

(4) The effect of loading rate was not consistent.

4.3 Rejection of the Initial (Study 27) Deformation Hypothesis: In order to test the original deformation hypothesis with the data presented above, it was necessary to limit the hypothesis to Equations 1 and 2, since the strain, ε_r, was not measured. Also, because the conditions of the triaxial test required that $\varepsilon_z = \varepsilon_\theta = 0$ when $\sigma_z = \sigma_r$, it was necessary to arbitrarily assign a value of 0.5 to k_1; otherwise this special condition would not be satisfied. Additionally, initial analysis of the data indicated anisotropic behavior, as evidenced by the fact that the ratios of simultaneous values of ε_θ and ε_z in nearly all cases exceed 0.5, the limiting value of homogeneous, isotropic mass. Therefore, the constants appearing in the denominator of Equation 2 could not be assumed to have the same values as the corresponding constants in Equation 1. With these restrictions, and with the assumption $\sigma_r = \sigma_\theta$, the original hypothesis is represented by the following equations:

$$\varepsilon_z = \frac{\sigma_z - \sigma_r}{k_2 + k_3\,(2\sigma_r)} \qquad (1a)$$

$$\varepsilon_\theta = -\frac{0.5\;(\sigma_z - \sigma_r)}{k_4 + k_5\,(\sigma_r + \sigma_z)} \qquad (2a)$$

It was found, as might have been expected from the work reported by Dunlap (1), that Equation 1a could be fitted to the ε_z data with fair accuracy. But all attempts to fit Equation 2a to the ε_θ data failed. As a result, the original hypothesis was rejected.

4.4 A New Hypothesis: A further study of the data led to a new hypothesis, expressed below:

$$\varepsilon_z = \frac{\sigma_z - 0.5\ (\sigma_r + \sigma_\theta)}{K_2 + K_3\ \sigma_r^2} \tag{4}$$

$$\varepsilon_\theta = \frac{\sigma_\theta - 0.5\ (\sigma_r + \sigma_z)}{K_4 + K_5\ \sigma_r^2} \tag{5}$$

With $\sigma_r = \sigma_\theta$, these equations reduce to the following:

$$\varepsilon_z = \frac{\sigma_z - \sigma_r}{K_2 + K_3\ \sigma_r^2} \tag{4a}$$

$$\varepsilon_\theta = -\ \frac{0.5\ (\sigma_z - \sigma_r)}{K_4 + K_5 \sigma_r^2} \tag{5a}$$

A non-linear, least-squares regression technique, developed by Moore and Milberger (5), was used with Equations 4a and 5a to determine the constants K_2, K_3, K_4 and K_5 for the four values of N at which tests were performed. A total of eight analyses were performed, the results of which are shown in Table 2. It may be seen from the generally high values of the correlation coefficient, R, given in the table, that Equations 4a and 5a are rather accurate models of the physical phenomena observed. This conclusion can be confirmed by referring to Figures 4 through 7, where the values of the constants K_2, K_3, K_4 and K_5 given in Table 2 have been used in Equations 4a and 5a to plot the

Table 2 : Results of Non-linear Regression Analyses

Analysis No.	Data Source		Average No. of Load Applications (millions)	Dependent Variable (mils/in.)	Constants Determined				Corr. Coeff., R	Root Mean Square Residual (mils/in)
	Table No.	Test No.			K2(ksi)	K3(1/ksi)	K4(ksi)	K5(1/ksi)		
1	B-1,B-2	1-6	0.06	ε_z	59.38	0.1120	--	--	0.99	0.021
2	B-1,B-2	1-6	0.06	ε_θ	--	--	11.04	0.0594	0.98	0.067
3	B-3,B-4	7-12	0.27	ε_z	85.85	0.1265	--	--	0.97	0.030
4	B-3,B-4	7-12	0.27	ε_θ	--	--	21.29	0.0664	0.99	0.037
5	B-5,B-6	13-18	0.77	ε_z	149.17	0.2147	--	--	0.97	0.016
6	B-5,B-6	13-18	0.77	ε_θ	--	--	42.35	0.2170	0.99	0.014
7	B-7,B-8	19-24	2.49	ε_z	311.59	0.2127	--	--	0.97	0.009
8	B-7,B-8	19-24	2.49	ε_θ	--	--	62.25	0.4448	0.99	0.008

Note: The model used in Analyses 1,3,5,7 was Equation 4a.
The model used in Analyses 2,4,6,8 was Equation 5a.
Forty-eight observations of the dependent variable were used in each analysis.

lines shown in the figures.

If σ_r is held constant, the modulus $K_2 + K_3 \sigma_r^2$, the slope of the axial stress-strain line, is analogous to the "resilient modulus" or "modulus of resilient deformation" sometimes estimated from a triaxial test performed at constant lateral pressure. It is interesting to note that equation 4a is somewhat similar to the hypothesis advanced by Seed and associates (7) who concluded that the modulus of resilient deformation of a dry granular material is directly proportional to either σ_c^n or to $(\sigma_z + \sigma_r + \sigma_\theta)^{n'}$.

<u>4.5 Effect of Accumulated Load Applications on the Modulus of the Material</u>: The expressions, $K_2 + K_3 \sigma_r^2$, and $K_4 + K_5 \sigma_r^2$, appearing in the denominators of Equations 4a and 5a, respectively, can each be regarded as a variable modulus of the material. For fixed values of σ_r and N, these moduli are determined by the constants K_2 and K_3 in the equation for ε_z, and K_4 and K_5 in the equation for ε_θ. It was found that these constants changed continuously during the testing program, as illustrated in Figures 8 and 9, where each constant has been plotted against the accumulated number of load applications at which it was determined.

Values of the resilient modulus for σ_r fixed at 30 psi, are given in Table 3, and are plotted in Figure 10 to illustrate the large increase in resilient modulus that occurred with increase in load applications.

A part of the increase in moduli occurring during the testing period can be attributed to a loss of about 0.7% (by dry weight) of moisture by the specimen during that period.

<u>4.6 Effect of Stress History on the Behavior of a Laboratory Specimen</u>: Whenever the specimen was not actually being tested, it was subjected to a deviator stress, $\sigma_z - \sigma_r$, of 34 psi every two seconds. The deviator stress

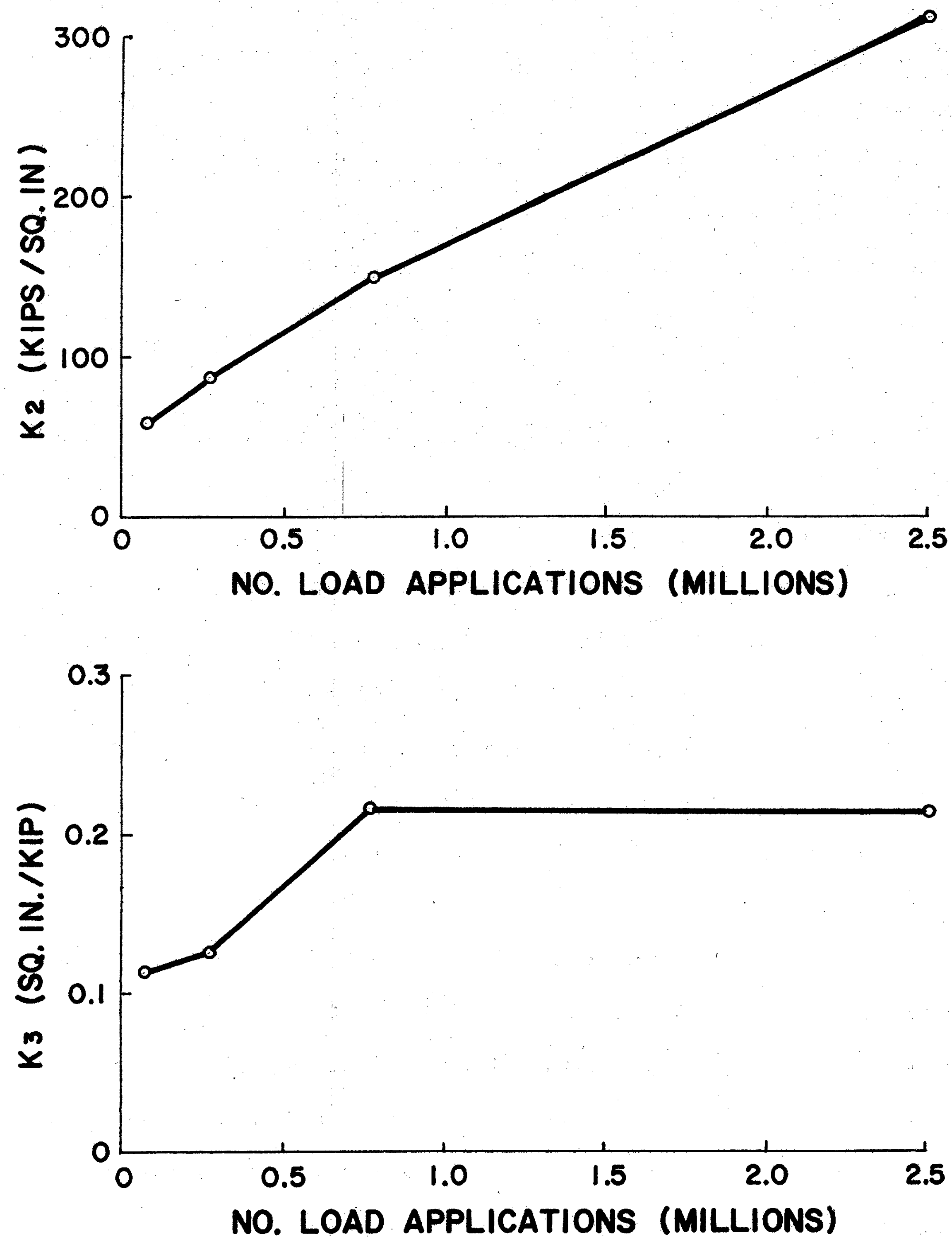

FIGURE 8 - Variation of the material parameters of Equation 4a with load applications. Some of this variation may have been due to a gradual loss of moisture.

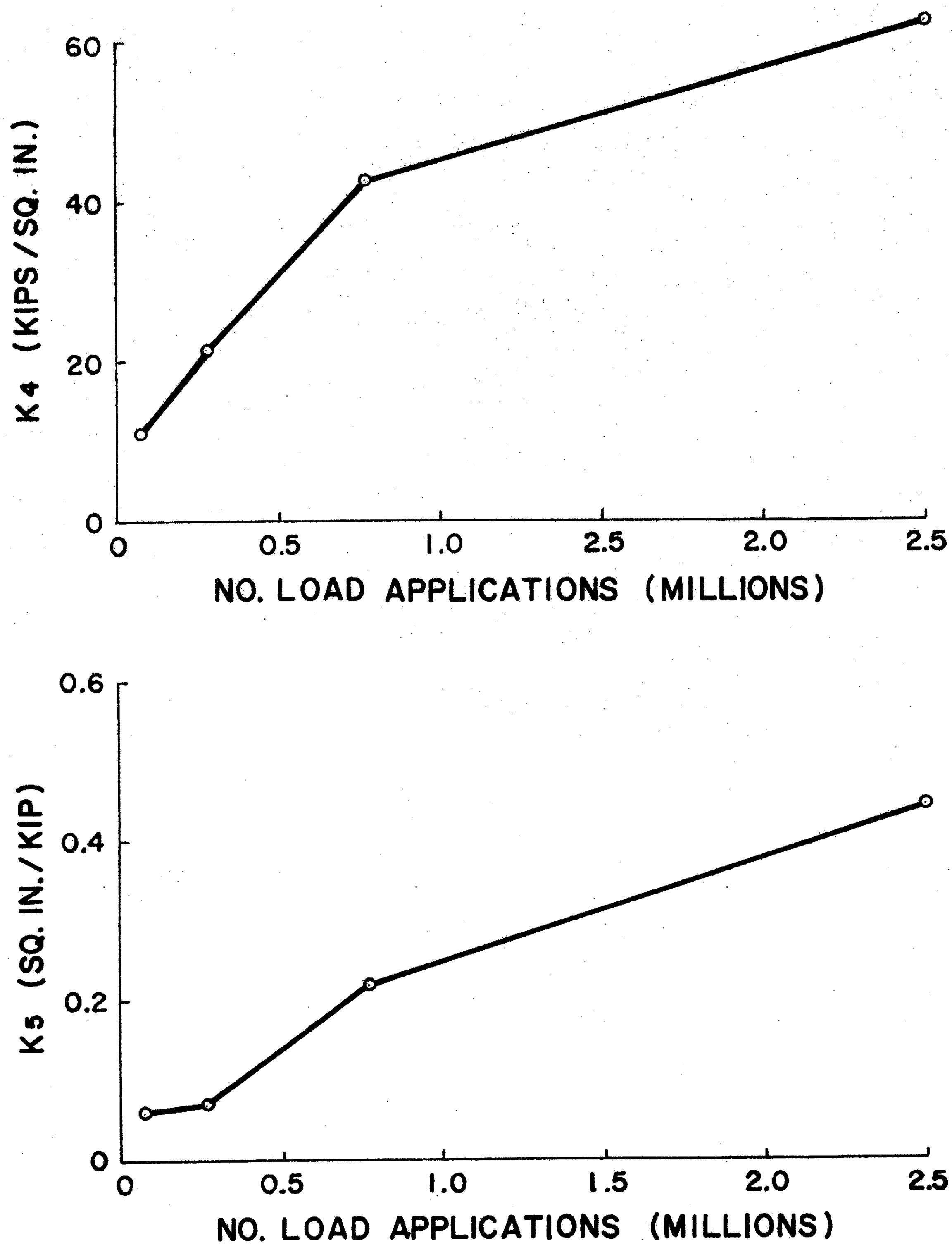

FIGURE 9 - Variation of the material parameters of Equation 5a with load applications. Some of this variation may have been due to a gradual loss of moisture.

Table 3: Resilient Modulus for A

Lateral Pressure of 30 psi

Test No.	Average No. of Load App's (millions)	Resilient * Modulus (psi) for σ_r = 30 psi
1-6	0.06	160,200
7-12	0.27	199,700
13-18	0.77	342,400
19-24	2.49	503,000

* Resilient Modulus (psi) $= 1000\ (K_2 + K_3\sigma_r^2)$.

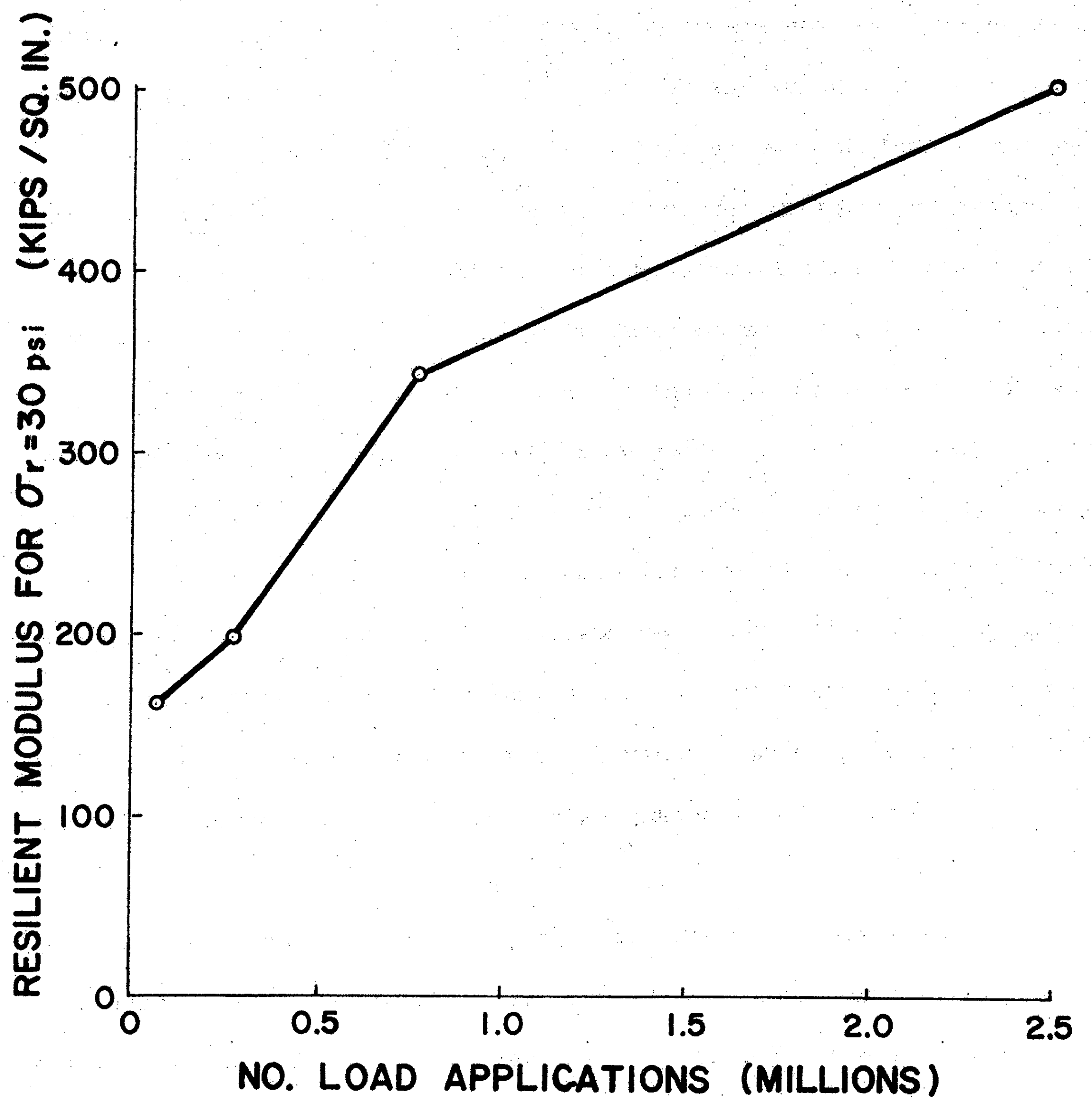

FIGURE 10 - Increase with load applications of the modulus $K_2 + K_3\sigma_r^2$, for σ_r = 30 psi.

was applied and released within the first 0.2 second of each two-second period after which the specimen "rested" for 1.8 seconds. The lateral pressure, σ_r, was held constant at 20 psi at all times excepting during those brief periods when testing at 10 psi or 30 psi was performed.

Testing periods were brief by intention: it was desired that the effect of a change in lateral pressure should be confounded with the gradual stiffening of the specimen that was known (from previous research) to occur as the result of large numbers of load applications (8).

The question arises: what would have been the effect on the stress-strain curves if - immediately after changing the lateral pressure to a value different from the conditioning pressure - several tests at the new lateral pressure were made in succession? Would they yield the same stress-strain curves (as was known to be the case with the testing lateral pressure at its conditioning value) or would the resilient modulus tend to change gradually - instead of instantaneously - following the change in lateral pressure?

A partial answer to those questions, for the case where the testing lateral pressure was <u>less</u> than the conditioning pressure, is provided by data acquired from a different, though nearly identical, specimen of the same material, conditioned for more than 400,000 applications at a lateral pressure of 20 psi, and then tested four times in rapid succession at a lateral pressure of 10 psi. The testing schedule is given in Table 4, and the stress-strain data are plotted in Figure 11.

It appears from Figure 11 that the specimen did, in fact, change substantially the brief testing period, as evidenced by the tendency of the slope of the stress-strain curve to decrease with each successive test. This is confirmed by Table 5, which gives the moduli, $K_2 + K_3\sigma_r^2$ and

Table 4: Testing Schedule,

Special Experiment

Load Appl. (millions) * From-To	Load Appl. (millions) * Increment	Beginning Date	Lateral Press. (psi)	Loading Rate	Test No.
0-0.332	0.332	5-5-70	20	Slow	None
0.332-0.417	0.085	5-13-70	20	Fast	None
0.417-0.419	0.002	5-15-70	10	Fast	None
0.419-0.420	0.001	5-15-70	10	Fast	25
0.420-0.424	0.004	5-15-70	10	Fast	None
0.424-0.425	0.001	5-15-70	10	Fast	26
0.425-0.426	0.001	5-15-70	10	Fast	None
0.426-0.427	0.001	5-15-70	10	Fast	27
0.427-0.428	0.001	5-15-70	10	Fast	None
0.428-0.429	0.001	5-15-70	10	Fast	28

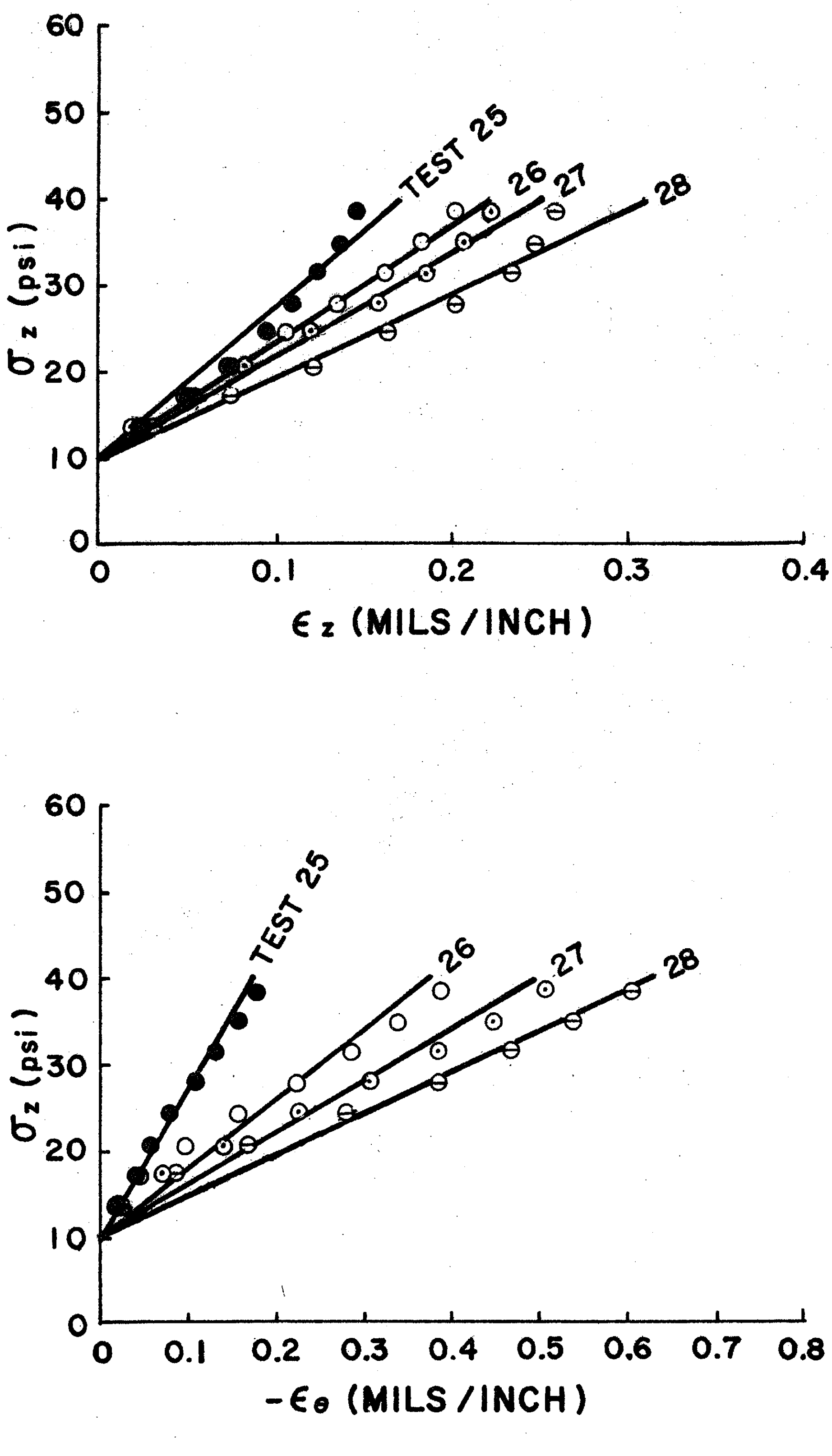

FIGURE 11 - Stress-strain data for special experiment.

Table 5: Modulii Computed From
Results of Special Experiment

Test No.	Mean Value of Load Appl. (millions)	Modulii (psi) *	
		$K_2 + K_3\sigma_r^2$	$K_4 + K_5\sigma_r^2$
25	0.4198	175,900	83,500
26	0.4248	136,800	38,600
27	0.4264	121,300	28,900
28	0.4280	97,300	23,900

* Computed from slopes of the regression lines in Figure 11, from following:

$$K_2 + K_3\sigma_r^2 = \frac{\partial\sigma_z}{\partial\varepsilon_z} \qquad \text{(N fixed)}$$

$$K_4 + K_5\sigma_r^2 = -\frac{1}{2}\frac{\partial\sigma_z}{\partial\varepsilon_\theta} \qquad \text{(N fixed)}$$

where $\partial\sigma_z/\partial\varepsilon_\theta$ is the slope of a line in the upper graph and $\partial\sigma_z/\partial\varepsilon_\theta$ is the slope of a line in the lower graph.

$K_4 + K_5\sigma_r^2$, for each of the four tests. Here, contrary to the data presented in Figure 10, we are confronted with an extremely rapid decrease in modulus as load applications are increased.

The tests represented in Figure 11 and in Table 5 were performed in May, 1970, as a part of Study 2-8-69-136, several months after Study 99 had been officially terminated. There has been little opportunity in Study 136 - which is concerned mainly with insitu testing - to pursue further the study of the effect of stress history on the behavior of a laboratory specimen. At this time it can only be said that the precise behavior of such a specimen is apparently influenced by all that has happened to it in the past. Thus, it seems that it may not be possible, even in a controlled environment, to predict with precision how a laboratory specimen of granular material will behave when loaded at a given point in time, unless its behavior at some past instant has been determined, and its entire stress history from that time to the present is known.

5. Conclusions

Neglecting the slight - though fairly consistent - curvature of the plotted stress-strain curves, the following conclusions were drawn from the analysis of the data acquired from the specimen tested in the main experiment:

(1) With N fixed, Equations 4_a and 5_a represent the observed phenomena with considerable accuracy; in other words, each strain, ε_z or ε_θ, was directly proportional to the deviator stress, σ_z or σ_r, and inversely proportional to the square of the radial stress plus a constant.

(2) The moduli, $K_2 + K_3\sigma_r^2$ and $K_4 + K_5\sigma_r^2$, increased as N increased.

(3) The fact that, with N fixed, $K_2 \neq K_4$ and $K_3 \neq K_5$, indicated that the specimen was anisotropic.

(4) The effect of loading rate was usually small and was not consistent.

(5) Unexpectedly high moduli were observed in this study which tend to confirm the high in situ values estimated from Dynaflect measurements made in Study 123, "A System Analysis of Pavement Design and Research Implementation." (A report of these estimates will be issued under Study 123).

In a special experiment made on a different but nearly identical specimen, conditioned in the same manner as the specimen used in the main experiment, it was found that the moduli decreased rapidly as N increased, when tests were made in rapid succession at a reduced lateral pressure. Thus, it seems that it may not be possible, even in a controlled environment, to predict with precision how a laboratory specimen of granular material will behave when at a given point in time, unless its behavior at some past instant has been determined, and its entire stress history from that time to the present is known. Accordingly, it appears that accurate predictions, on a routine basis, of traffic induced stresses and strains in a flexible pavement are not within reach, at least for the present.

6. REFERENCES

1. Dunlap, Wayne A. "A Mathematical Model Describing the Deformation Characteristics of Granular Materials," Research Report 27-1, Texas Transportation Institute, Texas A&M University, College Station, Texas, 1963, 44 pp.

2. Scrivner, Frank H. "An Extension of Elasticity Theory to Include Granular Materials," Research Report 27-2, Texas Transportation Institute, Texas A&M University, College Station, Texas, February, 1964, 13 pp.

3. Koehler, Albert Max, "Stress-Strain Properties of Soil-Aggregate Subjected to Rapid Loading," unpublished Doctor's Dissertation, Texas A&M University, College Station, Texas, 1964.

4. Moore, William M., Swift, Gilbert, and Milberger, Lionel J., "Deformation Measuring System for Repetitively Loaded, Large Diameter Specimens of Granular Materials," Research Report 99-4, Texas Transportation Institute, Texas A&M University, College Station, Texas, August, 1969, 30 pp.

5. Moore, William M., and Milberger, Lionel J., "Evaluation of The TTI Gyratory Compactor," Research Report 99-3, Texas Transportation Institute, Texas A&M University, College Station, Texas, February, 1968, 52 pp.

6. Milberger, Lionel J. and Dunlap, Wayne A., "A Gyratory Compactor For Molding Large Diameter Triaxial Specimens of Granular Materials," Research Report 99-2, Texas Transportation Institute, Texas A&M University, College Station, Texas, October, 1966, 229 pp.

7. Seed, H. B., Mitry, F. G., Monismith, C. L. and Chan, C. K., "Prediction of Flexible Pavement Deflections From Laboratory Repeated-Load Tests," NCHRP Report 35, 1967, 118 pp.

8. Dunlap, Wayne A., "Deformation Characteristics of Granular Materials Subjected to Rapid, Repetitive Loading," Research Report 27-4, Texas Transportation Institute, Texas A&M University, College Station, Texas, November, 1967, 209 pp.

Appendix A
Basic Test Data

This appendix contains the twenty-four tables of load-displacement data used for analysis. Each table represents a single test as described in Section 4 and illustrated by Figure 2. Each was prepared in the same manner as - and is similar to - Tables 3 and 4 of Research Report 99-4 (4). For a complete description of the equipment used and the data processing procedures employed for their preparation, the reader is referred to that report.

The values of the load shown in each table represent the measured vertical force applied to the loading rod of the triaxial apparatus. The values of z indicate the vertical distance measured downward from the top of the test specimen. Each vertical and radial displacement value is the average of four displacement component measurements made with a newly developed optical tracker, at the instant the load reached its indicated value. Two of the four measurements that were averaged were made at the same value of z but on the opposite side of the test specimen. This average is assumed to represent the displacement that would have been observed on the periphery of the specimen if the displacements had been perfectly axi-symmetric. Each value given for loading rate and rod displacement is the average of 36 values (two for each of the eighteen targets shown in Figure 1) determined at the instant the load reached its indicated value.

The basic data used to prepare the tables given in this appendix were digitized analog records of each test. These data are available on IBM computer cards.

Table A-1: Test Data for σ_r = 10 psi,
N = 0.04 millions, and Fast Loading Rate
Test 1

	LOAD (POUNDS)							
	100	200	300	400	500	600	700	800
z (in)				Vertical Displacement (mils)				
0*	0.598	1.738	2.975	4.084	4.977	5.662	6.182	6.638
1	0.408	1.171	2.111	2.890	3.533	4.035	4.476	4.830
2	0.386	1.048	1.744	2.401	2.886	3.257	3.588	3.876
3	0.372	0.974	1.734	2.357	2.872	3.279	3.582	3.803
4	0.303	0.775	1.394	1.974	2.405	2.760	3.063	3.291
5	0.354	0.886	1.522	2.069	2.528	2.867	3.153	3.398
6	0.276	0.764	1.366	1.916	2.366	2.719	3.020	3.255
7	0.187	0.585	0.863	1.180	1.382	1.550	1.684	1.823
8*	-0.000	0.019	0.034	0.045	0.058	0.074	0.086	0.102
				Radial Displacement (mils)				
0*	-0.011	0.016	0.030	0.044	0.045	0.033	0.049	0.049
1	0.019	0.118	0.274	0.409	0.535	0.632	0.701	0.769
2	0.054	0.238	0.478	0.754	1.023	1.212	1.358	1.494
3	0.129	0.434	0.887	1.325	1.693	1.987	2.233	2.435
4	0.112	0.446	0.968	1.526	1.989	2.344	2.631	2.829
5	0.175	0.517	1.046	1.503	1.878	2.173	2.427	2.624
6	0.099	0.332	0.662	0.997	1.274	1.484	1.670	1.807
7	0.031	0.138	0.240	0.381	0.492	0.590	0.676	0.752
8*	0.000	-0.000	-0.000	0.001	-0.001	-0.001	-0.001	-0.001
Loading Rate (pound/sec)	11500	14800	15100	15300	15500	14700	12800	8600
Rod Displacement (mils)	0.732	1.839	3.076	4.220	5.136	5.837	6.387	6.865

* Displacement shown for z = 0 and 8 in. is the displacement for the top loading plate and triaxial cell base respectively.

Table A-2: Test Data for σ_r = 20 psi,
N = 0.05 millions, and Fast Loading Rate
Test 2

	LOAD (POUNDS)							
	100	200	300	400	500	600	700	800
z (in)	Vertical Displacement (mils)							
0*	0.386	0.871	1.474	2.192	2.895	3.561	4.127	4.619
1	0.282	0.657	1.106	1.619	2.181	2.669	3.116	3.445
2	0.243	0.572	0.991	1.440	1.844	2.227	2.552	2.839
3	0.227	0.537	0.950	1.382	1.741	2.077	2.392	2.677
4	0.199	0.434	0.741	1.095	1.442	1.754	2.020	2.247
5	0.197	0.460	0.789	1.135	1.485	1.813	2.112	2.340
6	0.155	0.416	0.736	1.071	1.404	1.734	1.994	2.219
7	0.167	0.324	0.555	0.776	0.952	1.104	1.247	1.368
8*	0.007	0.017	0.030	0.046	0.055	0.058	0.077	0.096
	Radial Displacement (mils)							
0*	0.018	0.031	0.055	0.072	0.071	0.081	0.083	0.077
1	0.004	0.024	0.062	0.113	0.161	0.209	0.257	0.303
2	0.009	0.054	0.155	0.285	0.413	0.547	0.672	0.775
3	0.047	0.138	0.310	0.507	0.715	0.937	1.120	1.282
4	0.046	0.145	0.335	0.582	0.839	1.096	1.322	1.525
5	0.083	0.218	0.395	0.615	0.890	1.140	1.362	1.542
6	0.046	0.143	0.275	0.435	0.604	0.768	0.895	1.028
7	0.008	0.026	0.084	0.143	0.197	0.251	0.312	0.362
8*	-0.000	-0.000	-0.000	-0.001	-0.001	-0.002	-0.004	-0.007
Loading Rate (pounds/sec)	14200	17600	20000	19400	17300	16100	13800	8900
Rod Displacement (mils)	0.512	1.089	1.777	2.518	3.243	3.922	4.495	4.972

* Displacement shown for z = 0 and 8 in. is the displacement for the top loading plate and triaxial cell base respectively.

Table A-3: Test Data for σ_r = 30 psi,

N = 0.05 millions, and Fast Loading Rate

Test 3

z (in)	100	200	300	400	500	600	700	800
	LOAD (POUNDS)							
	Vertical Displacement (mils)							
0*	0.260	0.548	0.902	1.269	1.669	2.079	2.476	2.839
1	0.171	0.422	0.694	0.989	1.308	1.628	1.924	2.218
2	0.167	0.364	0.604	0.866	1.139	1.418	1.670	1.900
3	0.174	0.357	0.568	0.802	1.053	1.292	1.517	1.745
4	0.139	0.292	0.461	0.651	0.845	1.045	1.256	1.465
5	0.150	0.310	0.493	0.674	0.894	1.114	1.313	1.523
6	0.113	0.265	0.443	0.621	0.818	1.026	1.212	1.396
7	0.082	0.209	0.336	0.459	0.582	0.691	0.795	0.906
8*	0.022	0.030	0.039	0.051	0.063	0.073	0.084	0.103
	Radial Displacement (mils)							
0*	0.000	0.007	0.019	0.035	0.031	0.037	0.036	0.038
1	-0.006	-0.011	-0.010	-0.005	0.018	0.038	0.063	0.085
2	0.022	0.044	0.073	0.110	0.158	0.242	0.315	0.382
3	0.025	0.070	0.130	0.195	0.291	0.406	0.499	0.601
4	0.035	0.081	0.141	0.232	0.330	0.448	0.589	0.714
5	0.034	0.098	0.186	0.280	0.409	0.542	0.681	0.809
6	0.048	0.068	0.123	0.184	0.265	0.357	0.440	0.530
7	0.014	0.032	0.054	0.073	0.096	0.123	0.153	0.184
8*	-0.003	0.003	0.009	0.006	-0.003	-0.007	-0.002	-0.010
Loading Rate (pounds/sec)	13500	20600	22800	22700	20900	18600	15000	9300
Rod Displacement (mils)	0.344	0.720	1.127	1.547	1.987	2.436	2.872	3.256

* Displacement shown for z = 0 and 8 in. is the displacement for the top loading plate and triaxial cell base respectively.

Table A-4: Test Data for σ_r = 10 psi,

N = 0.06 millions, and Slow Loading Rate

Test 4

	LOAD (POUNDS)							
	100	200	300	400	500	600	700	800
z (in)				Vertical Displacement (mils)				
0*	0.570	1.512	2.629	3.605	4.294	4.882	5.315	5.668
1	0.386	1.113	1.909	2.604	3.126	3.510	3.820	4.056
2	0.319	0.876	1.527	2.064	2.469	2.794	3.036	3.258
3	0.282	0.754	1.405	1.891	2.260	2.545	2.745	2.951
4	0.208	0.683	1.198	1.644	1.993	2.252	2.434	2.617
5	0.220	0.699	1.232	1.708	2.031	2.272	2.455	2.619
6	0.206	0.644	1.167	1.602	1.940	2.193	2.389	2.533
7	0.181	0.446	0.715	0.881	1.047	1.126	1.222	1.283
8*	0.005	0.007	0.018	0.025	0.029	0.060	0.070	0.076
				Radial Displacement (mils)				
0*	0.017	0.050	0.075	0.088	0.092	0.089	0.094	0.088
1	0.021	0.078	0.186	0.287	0.378	0.440	0.491	0.535
2	0.038	0.178	0.444	0.671	0.873	1.004	1.116	1.210
3	0.064	0.293	0.707	1.081	1.357	1.590	1.767	1.911
4	0.110	0.363	0.833	1.295	1.653	1.905	2.102	2.271
5	0.108	0.423	0.874	1.294	1.589	1.832	2.005	2.150
6	0.050	0.232	0.532	0.799	0.983	1.134	1.253	1.365
7	0.035	0.093	0.209	0.305	0.422	0.472	0.536	0.579
8*	-0.005	-0.005	-0.005	-0.003	-0.009	-0.010	-0.010	-0.012
Loading Rate (pounds/sec)	2900	3300	3700	4600	4600	4800	5000	5100
Rod Displacement (mils)	0.589	1.556	2.681	3.601	4.281	4.836	5.267	5.610

* Displacement shown for z = 0 and 8 in. is the displacement for the top loading plate and triaxial cell base respectively.

Table A-5: Test Data for σ_r = 20 psi,
N = 0.06 millions, and Slow Loading Rate

Test 5

	LOAD (POUNDS)							
	100	200	300	400	500	600	700	800
z (in)	Vertical Displacement (mils)							
0*	0.324	0.779	1.315	1.869	2.466	3.056	3.490	3.875
1	0.250	0.626	1.007	1.464	1.915	2.328	2.696	2.972
2	0.211	0.518	0.878	1.248	1.623	1.945	2.246	2.470
3	0.215	0.494	0.793	1.117	1.453	1.738	2.003	2.225
4	0.167	0.405	0.648	0.929	1.223	1.472	1.700	1.870
5	0.180	0.415	0.677	0.964	1.220	1.483	1.716	1.900
6	0.148	0.355	0.622	0.883	1.138	1.386	1.592	1.753
7	0.125	0.277	0.420	0.581	0.731	0.836	0.921	1.002
8*	0.031	0.041	0.051	0.064	0.078	0.087	0.104	0.112
	Radial Displacement (mils)							
0*	0.025	0.039	0.046	0.065	0.080	0.101	0.105	0.103
1	-0.004	0.006	0.025	0.061	0.094	0.128	0.178	0.209
2	0.026	0.073	0.143	0.235	0.349	0.463	0.574	0.651
3	0.037	0.118	0.236	0.407	0.620	0.808	0.995	1.130
4	0.028	0.122	0.277	0.476	0.707	0.925	1.149	1.306
5	0.074	0.206	0.358	0.566	0.779	1.008	1.206	1.345
6	0.037	0.097	0.197	0.322	0.446	0.590	0.705	0.788
7	0.005	0.024	0.066	0.104	0.166	0.212	0.253	0.292
8*	0.009	0.014	0.018	0.009	0.006	0.009	0.004	0.009
Loading Rate (pounds/sec)	2900	3900	4300	4500	4700	4400	4400	4300
Rod Displacement (mils)	0.444	0.983	1.544	2.159	2.763	3.330	3.807	4.199

* Displacement shown for z = 0 and 8 in. is the displacement for the top loading plate and triaxial cell base respectively.

Table A-6: Test Data for σ_r = 30 psi,

N = 0.06 millions, and Slow Loading Rate

Test 6

	LOAD (POUNDS)							
	100	200	300	400	500	600	700	800
z (in)	Vertical Displacement (mils)							
0*	0.226	0.514	0.805	1.142	1.479	1.827	2.123	2.362
1	0.168	0.402	0.656	0.917	1.179	1.447	1.726	1.965
2	0.158	0.362	0.560	0.786	1.034	1.284	1.512	1.721
3	0.143	0.332	0.520	0.708	0.925	1.151	1.342	1.527
4	0.104	0.256	0.423	0.573	0.740	0.927	1.095	1.260
5	0.110	0.247	0.407	0.563	0.737	0.895	1.075	1.210
6	0.101	0.238	0.376	0.609	0.769	0.927	1.085	1.220
7	0.074	0.169	0.261	0.352	0.461	0.531	0.595	0.678
8*	0.016	0.027	0.041	0.054	0.067	0.077	0.086	0.102
	Radial Displacement (mils)							
0*	0.000	0.019	0.040	0.055	0.068	0.058	0.053	0.069
1	0.017	0.020	0.018	0.035	0.051	0.093	0.116	0.130
2	0.004	0.046	0.073	0.111	0.169	0.211	0.274	0.331
3	0.029	0.065	0.122	0.181	0.260	0.364	0.458	0.562
4	0.024	0.076	0.128	0.215	0.315	0.440	0.571	0.667
5	0.035	0.085	0.165	0.260	0.357	0.476	0.588	0.709
6	0.021	0.065	0.100	0.154	0.210	0.290	0.373	0.419
7	-0.004	0.008	0.031	0.048	0.068	0.086	0.106	0.134
8*	-0.010	-0.004	-0.009	-0.012	-0.009	-0.004	-0.008	-0.016
Loading Rate (pounds/sec)	2700	4100	4600	5000	4700	4500	4600	4500
Rod Displacement (mils)	0.344	0.734	1.114	1.493	1.878	2.287	2.660	2.992

* Displacement shown for z = 0 snd 8 in. is the displacement for the top loading plate and triaxial cell base respectively.

Table A-7: Test Data for σ_r = 30 psi

N = 0.24 millions, and Fast Loading Rate

Test 7

	LOAD (POUNDS)							
	100	200	300	400	500	600	700	800
z (in)	Vertical Displacement (mils)							
0*	0.198	0.449	0.713	1.002	1.296	1.618	1.935	2.249
1	0.140	0.340	0.544	0.766	0.998	1.250	1.493	1.723
2	0.143	0.325	0.538	0.739	0.948	1.166	1.354	1.539
3	0.133	0.289	0.462	0.651	0.847	1.037	1.212	1.378
4	0.115	0.255	0.412	0.577	0.733	0.882	1.034	1.174
5	0.092	0.213	0.349	0.492	0.667	0.843	1.007	1.154
6	0.112	0.242	0.388	0.544	0.690	0.841	1.008	1.172
7	0.084	0.176	0.299	0.432	0.549	0.652	0.744	0.826
8*	0.006	0.019	0.028	0.039	0.053	0.062	0.080	0.104
	Radial Displacement (mils)							
0*	-0.004	0.002	-0.005	0.001	0.016	0.018	0.017	0.025
1	-0.015	-0.020	-0.017	0.005	0.025	0.029	0.048	0.080
2	0.004	0.027	0.047	0.085	0.127	0.166	0.205	0.258
3	0.023	0.033	0.068	0.134	0.209	0.279	0.348	0.451
4	0.029	0.076	0.139	0.203	0.287	0.384	0.485	0.580
5	0.015	0.056	0.122	0.203	0.297	0.393	0.482	0.573
6	0.023	0.064	0.097	0.131	0.191	0.259	0.330	0.401
7	-0.005	-0.005	0.009	0.032	0.060	0.078	0.092	0.104
8*	0.010	0.010	0.010	0.010	0.010	0.010	0.010	0.010
Loading Rate (pounds/sec)	11200	14000	16900	16800	15600	12600	10200	5000
Rod Displacement (mils)	0.309	0.635	0.980	1.328	1.680	2.026	2.332	2.630

* Displacement shown for z = 0 and 8 in. is the displacement for the top loading plate and triaxial cell base respectively.

Table A-8: Test Data for σ_r = 20 psi,
N - 0.24 millions, and Fast Loading Rate
Test 8

	LOAD (POUNDS)							
	100	200	300	400	500	600	700	800
z (in)	Vertical Displacement (mils)							
0*	0.288	0.677	1.090	1.574	2.083	2.560	2.927	3.238
1	0.212	0.480	0.810	1.195	1.564	1.887	2.174	2.410
2	0.196	0.463	0.766	1.099	1.391	1.656	1.904	2.102
3	0.179	0.412	0.695	0.987	1.258	1.512	1.749	1.932
4	0.163	0.376	0.612	0.865	1.093	1.299	1.490	1.667
5	0.142	0.350	0.599	0.841	1.095	1.317	1.501	1.651
6	0.141	0.339	0.586	0.854	1.084	1.296	1.491	1.669
7	0.115	0.264	0.432	0.604	0.765	0.901	1.034	1.146
8*	0.011	0.021	0.034	0.048	0.062	0.073	0.087	0.107
	Radial Displacement (mils)							
0*	0.014	0.044	0.070	0.067	0.046	0.027	0.026	0.004
1	0.009	0.020	0.042	0.085	0.114	0.152	0.194	0.237
2	0.012	0.057	0.118	0.187	0.276	0.365	0.438	0.509
3	0.017	0.071	0.159	0.272	0.412	0.558	0.678	0.793
4	0.056	0.133	0.243	0.402	0.567	0.724	0.879	1.021
5	0.046	0.138	0.258	0.396	0.572	0.720	0.844	0.972
6	0.031	0.091	0.180	0.291	0.408	0.509	0.591	0.663
7	0.005	0.013	0.037	0.073	0.115	0.156	0.181	0.213
8*	0.000	0.000	0.000	0.000	0.000	0.000	0.002	0.005
Loading Rate (pounds/sec)	10500	14400	15500	15500	13600	12400	9600	4900
Rod Displacement (mils)	0.381	0.842	1.332	1.846	2.344	2.797	3.173	3.517

* Displacement shown for z = 0 and 8 in. is the displacement for the top loading plate and triaxial cell base respectively.

Table A-9: Test Data for σ_r = 10 psi,

N = 0.25 millions, and Fast Loading Rate

Test 9

	LOAD (POUNDS)							
	100	200	300	400	500	600	700	800
z (in)	Vertical Displacement (mils)							
0*	0.525	1.217	2.014	2.729	3.330	3.813	4.225	4.570
1	0.352	0.887	1.422	1.894	2.327	2.682	2.961	3.205
2	0.332	0.780	1.250	1.673	2.029	2.309	2.560	2.783
3	0.324	0.736	1.172	1.596	1.946	2.201	2.446	2.635
4	0.269	0.628	1.020	1.360	1.629	1.897	2.116	2.287
5	0.241	0.609	0.979	1.318	1.618	1.863	2.087	2.268
6	0.237	0.627	1.011	1.351	1.652	1.908	2.125	2.298
7	0.199	0.437	0.698	0.918	1.066	1.220	1.360	1.472
8*	0.010	0.023	0.035	0.042	0.054	0.069	0.079	0.089
	Radial Displacement (mils)							
0*	0.009	0.014	0.018	0.021	0.031	0.038	0.041	0.032
1	0.036	0.081	0.158	0.256	0.330	0.388	0.446	0.497
2	0.060	0.167	0.319	0.469	0.591	0.726	0.819	0.914
3	0.043	0.218	0.446	0.682	0.917	1.089	1.227	1.365
4	0.061	0.254	0.543	0.861	1.123	1.340	1.523	1.666
5	0.076	0.242	0.507	0.761	1.002	1.214	1.362	1.510
6	0.047	0.203	0.377	0.559	0.731	0.859	0.973	1.070
7	0.029	0.081	0.142	0.189	0.257	0.325	0.385	0.428
8*	0.000	0.000	0.000	0.000	0.000	0.000	0.000	0.000
Loading Rate (pounds/sec)	10400	12900	14200	14600	13600	12200	9400	4800
Rod Displacement (mils)	0.601	1.375	2.164	2.857	3.441	3.937	4.327	4.695

* Displacement shown for z = 0 and 8 in. is the displacement for the top loading plate and triaxial cell base respectively.

Table A-10: Test Data for σ_r = 30 psi,
N = 0.29 millions, and Slow Loading Rate

Test 10

	LOAD (POUNDS)							
	100	200	300	400	500	600	700	800
z (in)				Vertical Displacement (mils)				
0*	0.209	0.486	0.782	1.134	1.512	1.864	2.235	2.563
1	0.156	0.375	0.625	0.878	1.182	1.453	1.723	1.994
2	0.136	0.316	0.541	0.770	1.005	1.257	1.486	1.704
3	0.120	0.310	0.502	0.711	0.909	1.149	1.372	1.560
4	0.117	0.262	0.428	0.601	0.778	0.970	1.142	1.292
5	0.095	0.238	0.397	0.576	0.750	0.924	1.115	1.271
6	0.107	0.250	0.378	0.558	0.720	0.886	1.066	1.197
7	0.090	0.193	0.288	0.409	0.506	0.643	0.743	0.826
8*	0.015	0.011	0.023	0.035	0.052	0.058	0.070	0.086
				Radial Displacement (mils)				
0*	0.031	0.046	0.053	0.042	0.064	0.061	0.050	0.065
1	-0.004	-0.026	-0.019	0.000	0.005	0.040	0.060	0.087
2	0.018	0.028	0.048	0.083	0.134	0.194	0.257	0.327
3	0.029	0.037	0.098	0.172	0.260	0.351	0.481	0.610
4	0.024	0.050	0.113	0.188	0.308	0.428	0.558	0.671
5	0.034	0.056	0.145	0.216	0.319	0.432	0.550	0.664
6	0.006	0.045	0.087	0.144	0.199	0.280	0.360	0.427
7	0.041	0.056	0.057	0.077	0.105	0.136	0.176	0.200
8*	-0.002	0.000	-0.005	0.000	0.000	0.000	0.000	0.000
Loading Rate (pounds/sec)	2700	4300	5700	6500	6700	7000	6900	7000
Rod Displacement (mils)	0.289	0.642	1.012	1.399	1.786	2.188	2.580	2.937

* Displacement shown for z = 0 and 8 in. is the displacement for the top loading plate and triaxial cell base respectively.

Table A-11: Test Data for σ_r = 20 psi,
N = 0.29 millions, and Slow Loading Rate

Test 11

	LOAD (POUNDS)							
	100	200	300	400	500	600	700	800
z (in)				Vertical Displacement (mils)				
0*	0.313	0.672	1.136	1.653	2.151	2.648	3.013	3.356
1	0.223	0.520	0.876	1.294	1.656	2.051	2.334	2.625
2	0.208	0.498	0.846	1.239	1.590	1.945	2.192	2.454
3	0.193	0.465	0.771	1.102	1.397	1.681	1.912	2.127
4	0.172	0.404	0.657	0.961	1.227	1.477	1.688	1.902
5	0.147	0.344	0.570	0.848	1.103	1.347	1.538	1.723
6	0.121	0.319	0.580	0.832	1.101	1.316	1.524	1.676
7	0.102	0.248	0.419	0.592	0.732	0.851	0.948	1.017
8*	0.024	0.025	0.043	0.050	0.070	0.082	0.101	0.113
				Radial Displacement (mils)				
0*	0.026	0.047	0.074	0.068	0.063	0.065	0.066	0.078
1	-0.002	0.007	0.002	0.035	0.092	0.142	0.180	0.210
2	0.034	0.075	0.125	0.208	0.331	0.430	0.514	0.600
3	0.030	0.088	0.204	0.372	0.541	0.744	0.889	1.017
4	0.030	0.119	0.259	0.434	0.640	0.864	1.026	1.197
5	0.019	0.126	0.225	0.383	0.549	0.723	0.879	1.014
6	0.039	0.101	0.190	0.303	0.404	0.523	0.639	0.729
7	-0.003	0.022	0.058	0.098	0.137	0.195	0.250	0.284
8*	-0.001	0.002	-0.001	0.001	0.008	0.007	-0.011	-0.008
Loading Rate (pounds/sec)	2800	4400	5800	6200	6600	6900	6500	6200
Rod Displacement (mils)	0.372	0.844	1.386	1.976	2.538	3.045	3.478	3.878

*Displacement shown for z = 0 and 8 in. is the displacement for the top loading plate and triaxial cell base respectively.

Table A-12: Test Data for σ_r = 10 psi,
N = 0.29 millions, and Slow Loading Rate

Test 12

	LOAD (POUNDS)							
	100	200	300	400	500	600	700	800
z (in)	Vertical Displacement (mils)							
0*	0.512	1.227	1.996	2.681	3.189	3.662	4.061	4.395
1	0.365	0.911	1.517	2.011	2.405	2.767	3.072	3.307
2	0.343	0.826	1.334	1.757	2.116	2.391	2.655	2.860
3	0.320	0.743	1.189	1.566	1.901	2.166	2.384	2.580
4	0.312	0.690	1.171	1.586	1.892	2.181	2.384	2.582
5	0.197	0.528	0.897	1.210	1.503	1.729	1.893	2.042
6	0.206	0.548	0.912	1.255	1.503	1.745	1.914	2.045
7	0.143	0.370	0.632	0.800	0.948	1.046	1.139	1.202
8*	0.005	0.011	0.026	0.040	0.051	0.055	0.067	0.074
	Radial Displacement (mils)							
0*	0.018	0.059	0.050	0.092	0.091	0.092	0.091	0.094
1	-0.029	-0.020	0.035	0.096	0.166	0.239	0.284	0.335
2	0.052	0.149	0.286	0.429	0.582	0.683	0.774	0.844
3	0.071	0.203	0.426	0.650	0.889	1.053	1.195	1.310
4	0.102	0.280	0.589	0.902	1.160	1.365	1.556	1.697
5	0.056	0.223	0.457	0.706	0.930	1.103	1.236	1.350
6	0.060	0.184	0.356	0.526	0.684	0.816	0.909	0.989
7	0.016	0.068	0.152	0.226	0.295	0.362	0.419	0.460
8*	-0.020	-0.008	-0.001	-0.009	0.007	0.007	-0.003	0.007
Loading Rate (pounds/sec)	2700	4200	5500	6400	6600	7100	6700	6500
Rod Displacement (mils)	0.553	1.318	2.145	2.843	3.420	3.882	4.282	4.632

*Displacement shown for z = 0 and 8 in. is the displacement for the top loading plate and triaxial cell base respectively.

Table A-13: Test Data for σ_r = 10 psi,

N = 0.73 millions, and Fast Loading Rate

Test 13

	LOAD (POUNDS)							
	100	200	300	400	500	600	700	800
z (in)				Vertical Displacement (mils)				
0*	0.353	0.803	1.228	1.614	1.932	2.227	2.497	2.725
1	0.224	0.565	0.902	1.210	1.456	1.664	1.844	2.008
2	0.230	0.534	0.860	1.119	1.331	1.510	1.666	1.769
3	0.209	0.468	0.740	0.960	1.164	1.344	1.493	1.605
4	0.188	0.428	0.650	0.856	1.038	1.205	1.341	1.444
5	0.174	0.405	0.642	0.849	1.021	1.164	1.302	1.403
6	0.189	0.406	0.623	0.815	0.989	1.106	1.205	1.278
7	0.115	0.249	0.398	0.509	0.595	0.659	0.700	0.727
8*	0.001	0.014	0.030	0.043	0.054	0.067	0.091	0.110
				Radial Displacement (mils)				
0*	0.017	-0.009	0.015	0.053	0.056	0.061	0.059	0.061
1	0.015	0.060	0.064	0.091	0.121	0.159	0.191	0.229
2	0.054	0.097	0.167	0.254	0.323	0.387	0.447	0.485
3	0.035	0.091	0.195	0.301	0.415	0.511	0.582	0.638
4	0.040	0.104	0.221	0.338	0.357	0.579	0.668	0.746
5	0.021	0.099	0.222	0.347	0.469	0.563	0.645	0.729
6	0.053	0.120	0.187	0.265	0.337	0.405	0.478	0.541
7	0.001	-0.022	-0.027	-0.027	-0.026	-0.025	-0.037	-0.935
8*	-0.003	-0.003	-0.003	-0.003	-0.004	-0.005	-0.010	-0.018
Loading Rate (pounds/sec)	8900	14200	17300	18700	18600	17400	15300	11800
Rod Displacement (mils)	0.455	0.989	1.480	1.913	2.282	2.583	2.847	3.056

*Displacement shown for z = 0 and 8 in. is the displacement for the top loading plate and triaxial cell base respectively.

Table A-14: Test Data for σ_r = 20 psi,

N = 0.73 millions, and Fast Loading Rate

Test 14

z (in)	LOAD (POUNDS) 100	200	300	400	500	600	700	800
				Vertical Displacement (mils)				
0*	0.201	0.437	0.684	0.928	1.161	1.384	1.607	1.792
1	0.160	0.361	0.545	0.731	0.922	1.184	1.319	1.432
2	0.148	0.305	0.493	0.683	0.837	0.981	1.118	1.240
3	0.129	0.285	0.445	0.607	0.759	0.884	1.001	1.116
4	0.120	0.265	0.394	0.517	0.645	0.761	0.878	0.975
5	0.117	0.260	0.406	0.532	0.642	0.765	0.875	0.958
6	0.103	0.229	0.362	0.485	0.599	0.713	0.817	0.894
7	0.068	0.165	0.261	0.333	0.408	0.479	0.539	0.589
8*	0.012	0.024	0.033	0.043	0.054	0.064	0.077	0.083
				Radial Displacement (mils)				
0*	0.012	0.030	0.059	0.058	0.049	0.041	0.042	0.027
1	0.011	0.035	0.045	0.044	0.054	0.070	0.100	0.121
2	0.011	0.020	0.032	0.057	0.096	0.143	0.173	0.209
3	0.005	0.039	0.052	0.093	0.143	0.199	0.251	0.304
4	0.019	0.029	0.086	0.151	0.226	0.283	0.339	0.387
5	0.016	0.071	0.097	0.136	0.200	0.270	0.343	0.396
6	0.019	0.043	0.074	0.116	0.162	0.207	0.246	0.279
7	-0.011	0.001	0.022	0.034	0.052	0.087	0.114	0.123
8*	0.000	-0.000	-0.002	-0.003	-0.003	-0.002	-0.000	-0.000
Loading Rate (pounds/sec)	9400	16100	18400	20300	19900	18700	16400	13100
Rod Displacement (mils)	0.288	0.634	0.948	1.235	1.509	1.755	1.968	2.167

* Displacement shown for z = 0 and 8 in. is the displacement for the top loading plate and triaxial cell base respectively.

Table A-15: Test Data for σ_r = 30 psi,

N = 0.73 millions, and Fast Loading Rate

Test 15

	LOAD (POUNDS)							
	100	200	300	400	500	600	700	800
z (in)	Vertical Displacement (mils)							
0*	0.167	0.331	0.543	0.715	0.864	1.003	1.147	1.282
1	0.124	0.301	0.446	0.580	0.713	0.844	0.957	1.075
2	0.121	0.246	0.385	0.504	0.612	0.729	0.853	0.960
3	0.073	0.182	0.294	0.400	0.500	0.606	0.710	0.802
4	0.089	0.166	0.264	0.372	0.464	0.545	0.627	0.704
5	0.071	0.166	0.275	0.364	0.450	0.533	0.610	0.679
6	0.061	0.153	0.239	0.322	0.408	0.500	0.588	0.641
7	0.051	0.107	0.171	0.231	0.279	0.325	0.383	0.435
8*	0.006	0.017	0.029	0.041	0.053	0.064	0.073	0.074
0*	-0.004	-0.004	-0.004	-0.003	0.001	-0.001	-0.001	-0.011
1	0.001	-0.005	-0.002	0.009	0.027	0.037	0.037	0.042
2	0.005	0.011	0.027	0.044	0.060	0.074	0.085	0.104
3	0.033	0.056	0.080	0.098	0.129	0.163	0.184	0.217
4	0.008	0.029	0.042	0.061	0.095	0.133	0.175	0.226
5	0.008	0.029	0.056	0.089	0.117	0.145	0.182	0.225
6	-0.000	0.011	0.038	0.064	0.097	0.116	0.133	0.177
7	-0.002	-0.001	0.004	0.010	0.023	0.037	0.052	0.066
8*	-0.002	-0.003	-0.002	-0.002	-0.004	-0.010	-0.010	-0.010
Loading Rate (pounds/sec)	9700	14700	18900	21300	21400	19600	17000	12600
Rod Displacement (mils)	0.222	0.515	0.777	0.990	1.190	1.371	1.529	1.693

*Displacement shown for z = 0 and 8 in. is the displacement for the top loading plate and triaxial cell base respectively.

Table A-16: Test Data for σ_r = 10 psi, N = 0.80 millions, and Slow Loading Rate

Test 16

z (in)	LOAD (POUNDS) 100	200	300	400	500	600	700	800
	Vertical Displacement (mils)							
0*	0.281	0.738	1.119	1.491	1.806	2.102	2.313	2.505
1	0.214	0.528	0.821	1.104	1.364	1.558	1.722	1.877
2	0.203	0.464	0.739	0.966	1.152	1.322	1.460	1.569
3	0.183	0.464	0.720	0.943	1.123	1.281	1.415	1.526
4	0.177	0.411	0.630	0.832	1.002	1.130	1.250	1.333
5	0.168	0.363	0.592	0.766	0.952	1.081	1.203	1.276
6	0.135	0.367	0.565	0.752	0.912	1.048	1.154	1.252
7	0.121	0.257	0.403	0.524	0.620	0.712	0.796	0.847
8*	0.016	0.012	0.029	0.037	0.048	0.058	0.074	0.048
	Radial Displacement (mils)							
0*	0.023	0.035	0.044	0.055	0.063	0.071	0.060	0.057
1	-0.003	0.007	0.032	0.071	0.074	0.121	0.153	0.186
2	0.013	0.038	0.106	0.174	0.262	0.320	0.355	0.402
3	0.010	0.069	0.166	0.237	0.357	0.456	0.529	0.582
4	0.035	0.106	0.212	0.334	0.451	0.542	0.626	0.688
5	0.041	0.102	0.201	0.330	0.427	0.522	0.603	0.641
6	0.013	0.076	0.152	0.227	0.285	0.355	0.397	0.430
7	0.002	0.017	0.050	0.075	0.133	0.167	0.197	0.222
8*	0.000	0.000	0.000	-0.000	-0.000	-0.000	-0.001	0.001
Loading Rate (pounds/sec)	2000	3600	4700	5500	5700	5900	6200	6000
Rod Displacement (mils)	0.352	0.821	1.280	1.922	2.049	2.362	2.607	2.795

*Displacement shown for z = 0 and 8 in. is the displacement for the top loading plate and triaxial cell base respectively.

Table A-17: Test Data for σ_r = 20 psi,
N = 0.81 millions, and Slow Loading Rate

Test 17

	LOAD (POUNDS)							
	100	200	300	400	500	600	700	800
z (in)	Vertical Displacement (mils)							
0*	0.173	0.394	0.623	0.840	1.067	1.285	1.484	1.666
1	0.102	0.276	0.442	0.620	0.808	0.976	1.134	1.273
2	0.110	0.259	0.416	0.591	0.734	0.886	1.029	1.135
3	0.116	0.280	0.409	0.555	0.697	0.844	0.956	1.075
4	0.093	0.222	0.346	0.497	0.617	0.721	0.844	0.935
5	0.086	0.208	0.325	0.447	0.550	0.674	0.770	0.861
6	0.085	0.203	0.330	0.437	0.561	0.670	0.763	0.838
7	0.070	0.155	0.247	0.347	0.419	0.476	0.543	0.597
8*	0.003	0.018	0.021	0.028	0.037	0.044	0.062	0.070
	Radial Displacement (mils)							
0*	-0.001	-0.001	0.001	0.019	0.017	0.035	0.026	0.019
1	0.006	0.018	0.036	0.045	0.050	0.077	0.104	0.124
2	-0.011	0.009	0.047	0.063	0.086	0.135	0.170	0.193
3	0.012	0.038	0.062	0.102	0.155	0.205	0.260	0.312
4	0.020	0.065	0.094	0.131	0.200	0.258	0.306	0.371
5	0.017	0.040	0.077	0.126	0.171	0.243	0.300	0.365
6	0.015	0.046	0.061	0.085	0.137	0.184	0.209	0.254
7	0.003	0.006	0.023	0.040	0.050	0.076	0.108	0.113
8*	0.003	0.014	0.014	0.014	0.014	0.017	0.016	0.016
Loading Rate (pounds/sec)	2200	3800	4800	5600	5900	5800	5900	5700
Rod Displacement (mils)	0.249	0.535	0.849	1.132	1.382	1.641	1.864	2.057

*Displacement shown for z = 0 and 8 in. is the displacement for the top loading plate and triaxial cell base respectively.

Table A-18: Test Data for σ_r = 30 psi,
N = 0.81 millions, and Slow Loading Rate

Test 18

	LOAD (POUNDS)							
	100	200	300	400	500	600	700	800
z (in)	Vertical Displacement (mils)							
0*	0.119	0.274	0.444	0.593	0.741	0.897	1.049	1.186
1	0.095	0.234	0.358	0.481	0.616	0.739	0.863	0.983
2	0.071	0.226	0.322	0.431	0.549	0.670	0.767	0.869
3	0.089	0.210	0.304	0.408	0.511	0.608	0.694	0.795
4	0.071	0.176	0.265	0.357	0.443	0.536	0.618	0.701
5	0.067	0.146	0.214	0.301	0.384	0.461	0.543	0.621
6	0.069	0.155	0.232	0.314	0.394	0.468	0.542	0.610
7	0.057	0.123	0.183	0.228	0.285	0.338	0.379	0.415
8*	0.015	0.018	0.032	0.055	0.066	0.079	0.088	0.097
	Radial Displacement (mils)							
0*	-0.019	-0.003	0.003	0.001	0.014	0.011	0.015	-0.000
1	-0.004	0.008	0.008	0.026	0.034	0.056	0.056	0.063
2	-0.001	0.012	0.015	0.028	0.042	0.067	0.089	0.106
3	0.010	0.025	0.058	0.068	0.097	0.117	0.137	0.175
4	0.048	0.056	0.076	0.093	0.119	0.135	0.183	0.205
5	0.015	0.044	0.058	0.067	0.097	0.134	0.178	0.204
6	0.005	0.027	0.031	0.042	0.068	0.081	0.098	0.138
7	0.001	0.026	0.019	0.029	0.035	0.045	0.046	0.058
8*	-0.002	-0.004	0.006	0.004	0.002	0.002	0.000	0.001
Loading Rate (pounds/sec)	2000	3400	4800	5500	5800	5800	6000	5600
Rod Displacement (mils)	0.207	0.453	0.703	0.930	1.120	1.319	1.503	1.649

*Displacement shown for z = 0 and 8 in. is the displacement for the top loading plate and triaxial cell base respectively.

Table A-19: Test Data for σ_r = 30 psi, N = 2.49 millions, and Fast Loading Rate

Test 19

	LOAD (POUNDS)							
	100	200	300	400	500	600	700	800
z (in)	Vertical Displacement (mils)							
0*	0.116	0.212	0.344	0.473	0.586	0.699	0.806	0.915
1	0.088	0.175	0.275	0.382	0.474	0.566	0.656	0.744
2	0.087	0.180	0.278	0.363	0.430	0.499	0.570	0.659
3	0.083	0.168	0.245	0.319	0.394	0.470	0.532	0.606
4	0.063	0.116	0.190	0.257	0.332	0.408	0.471	0.539
5	0.036	0.085	0.143	0.199	0.263	0.327	0.396	0.471
6	0.052	0.126	0.173	0.221	0.280	0.338	0.391	0.462
7	0.043	0.086	0.128	0.176	0.221	0.265	0.312	0.354
8*	0.007	0.024	0.046	0.051	0.058	0.078	0.089	0.108
	Radial Displacement (mils)							
0*	-0.014	-0.023	-0.015	-0.012	-0.020	-0.026	-0.024	-0.035
1	0.002	0.003	0.004	0.006	0.020	0.031	0.032	0.039
2	-0.002	0.007	0.017	0.024	0.035	0.043	0.043	0.052
3	0.001	0.013	0.021	0.034	0.048	0.070	0.080	0.082
4	-0.001	0.009	0.019	0.036	0.058	0.080	0.112	0.116
5	0.012	0.014	0.034	0.045	0.062	0.089	0.117	0.130
6	0.002	0.008	0.012	0.027	0.044	0.059	0.077	0.094
7	-0.001	0.006	0.008	0.011	0.016	0.023	0.028	0.041
8*	-0.000	-0.001	-0.002	-0.002	-0.002	-0.003	-0.003	-0.004
Loading Rate (pounds/sec)	10100	14000	17500	18800	18400	15700	12700	6100
Rod Displacement (mils)	0.395	0.634	0.819	0.997	1.160	1.312	1.472	1.660

*Displacement shown for z = 0 and 8 in. is the displacement for the top loading plate and triaxial cell base respectively.

Table A-20: Test Data for σ_r = 20 psi,

N = 2.49 millions, and Fast Loading Rate

Test 20

	LOAD (POUNDS)							
	100	200	300	400	500	600	700	800
z (in)	Vertical Displacement (mils)							
0*	0.193	0.353	0.513	0.686	0.862	1.007	1.144	1.269
1	0.106	0.231	0.372	0.516	0.643	0.757	0.865	0.971
2	0.114	0.239	0.369	0.494	0.608	0.713	0.800	0.879
3	0.116	0.250	0.383	0.491	0.598	0.689	0.774	0.848
4	0.087	0.188	0.303	0.408	0.496	0.585	0.664	0.735
5	0.092	0.196	0.300	0.393	0.490	0.583	0.656	0.718
6	0.078	0.163	0.249	0.322	0.397	0.473	0.554	0.626
7	0.087	0.171	0.254	0.332	0.401	0.453	0.511	0.574
8*	0.026	0.042	0.062	0.077	0.085	0.096	0.104	0.112
	Radial Displacement (mils)							
0*	0.008	-0.004	-0.012	-0.020	-0.026	-0.028	-0.023	-0.035
1	0.002	0.011	0.026	0.045	0.052	0.057	0.065	0.069
2	-0.001	0.002	0.008	0.027	0.045	0.054	0.068	0.085
3	0.005	0.023	0.053	0.078	0.104	0.118	0.135	0.140
4	0.014	0.018	0.040	0.079	0.118	0.144	0.166	0.199
5	0.011	0.026	0.064	0.114	0.138	0.163	0.180	0.196
6	0.002	0.024	0.033	0.054	0.082	0.104	0.122	0.142
7	-0.007	-0.001	-0.006	-0.002	0.006	0.021	0.047	0.069
8*	-0.001	-0.001	-0.002	-0.003	-0.005	-0.006	-0.007	-0.007
Loading Rate (pounds/sec)	10300	15100	19000	20200	19300	17800	13100	7600
Rod Displacement (mils)	0.438	0.770	1.027	1.233	1.425	1.593	1.776	1.987

* Displacement shown for z = 0 and 8 in. is the displacement for the top loading plate and triaxial cell base respectively.

Table A-21: Test Data for σ_r = 10 psi,
N = 2.49 millions, and Fast Loading Rate
Test 21

	LOAD (POUNDS)							
	100	200	300	400	500	600	700	800
z (in)	Vertical Displacement (mils)							
0*	0.338	0.652	0.952	1.261	1.522	1.734	1.910	2.069
1	0.227	0.450	0.716	0.928	1.111	1.280	1.417	1.525
2	0.188	0.405	0.628	0.825	0.995	1.142	1.272	1.370
3	0.212	0.418	0.599	0.791	0.966	1.125	1.237	1.330
4	0.183	0.364	0.547	0.708	0.860	0.993	1.112	1.214
5	0.186	0.346	0.513	0.679	0.820	0.942	1.041	1.143
6	0.155	0.316	0.493	0.652	0.787	0.875	0.961	1.065
7	0.158	0.336	0.498	0.590	0.692	0.795	0.865	0.925
8*	0.011	0.031	0.055	0.068	0.079	0.092	0.102	0.116
	Radial Displacement (mils)							
0*	0.008	0.011	0.014	0.011	0.010	0.014	0.008	0.007
1	0.003	0.024	0.047	0.057	0.079	0.088	0.101	0.125
2	0.010	0.032	0.100	0.149	0.180	0.215	0.249	0.284
3	0.009	0.065	0.118	0.173	0.230	0.290	0.333	0.373
4	0.013	0.072	0.129	0.185	0.253	0.327	0.377	0.416
5	0.016	0.065	0.124	0.184	0.249	0.318	0.375	0.432
6	0.010	0.046	0.090	0.140	0.201	0.251	0.295	0.334
7	-0.007	-0.008	-0 003	0.010	0.025	0.047	0.069	0.093
8*	-0.000	-0.001	-0.000	0.003	0.004	0.004	0.000	-0.004
Loading Rate (pounds/sec)	9500	15000	18400	19100	18700	17800	15100	8600
Rod Displacement (mils)	0.591	1.066	1.452	1.770	2.052	2.287	2.506	2.730

* Displacement shown for z = 0 and 8 in. is the displacement for the top loading plate and triaxial cell base respectively.

Table A-22: Test Data for σ_r = 30 psi,
N = 2.50 millions, and Slow Loading Rate
Test 22

	LOAD (POUNDS)							
	100	200	300	400	500	600	700	800
z (in)	Vertical Displacement (mils)							
0*	0.107	0.222	0.341	0.470	0.584	0.703	0.816	0.923
1	0.086	0.184	0.271	0.374	0.474	0.565	0.668	0.756
2	0.082	0.169	0.256	0.344	0.516	0.499	0.593	0.663
3	0.086	0.169	0.258	0.337	0.436	0.510	0.586	0.665
4	0.071	0.149	0.221	0.321	0.395	0.453	0.525	0.585
5	0.056	0.128	0.200	0.266	0.331	0.396	0.464	0.517
6	0.053	0.117	0.187	0.250	0.326	0.379	0.435	0.496
7	0.060	0.111	0.153	0.217	0.279	0.317	0.367	0.406
8*	0.023	0.040	0.060	0.067	0.089	0.097	0.106	0.114
	Radial Displacement (mils)							
0*	0.010	0.007	-0.004	-0.012	-0.008	-0.010	-0.016	-0.018
1	0.002	0.004	0.006	0.023	0.025	0.030	0.049	0.057
2	0.010	0.010	0.014	0.029	0.041	0.052	0.053	0.073
3	0.009	0.009	0.017	0.032	0.048	0.062	0.082	0.096
4	0.009	0.016	0.017	0.043	0.076	0.079	0.083	0.109
5	0.020	0.019	0.031	0.051	0.074	0.090	0.113	0.122
6	-0.002	0.007	0.025	0.028	0.040	0.054	0.066	0.085
7	-0.003	-0.003	0.001	0.002	0.026	0.030	0.041	0.044
8*	-0.001	-0.001	-0.002	-0.002	-0.003	-0.004	-0.004	-0.004
Loading Rate (pounds/sec)	2800	4500	5500	6200	5900	5700	4900	4200
Rod Displacement (mils)	0.289	0.540	0.755	0.961	1.130	1.299	1.463	1.647

* Displacement shown for z = 0 and 8 in. is the displacement for the top loading plate and triaxial cell base respectively.

Table A-23: Test Data for σ_r = 20 psi,

N = 2.50 millions, and Slow Loading Rate

Test 23

	LOAD (POUNDS)							
	100	200	300	400	500	600	700	800
z (in)				Vertical Displacement (mils)				
0*	0.158	0.312	0.488	0.674	0.840	0.984	1.153	1.299
1	0.110	0.238	0.378	0.513	0.650	0.772	0.895	0.998
2	0.082	0.220	0.331	0.445	0.566	0.678	0.776	0.874
3	0.093	0.214	0.322	0.433	0.557	0.657	0.758	0.851
4	0.101	0.208	0.302	0.418	0.527	0.619	0.700	0.785
5	0.084	0.166	0.270	0.361	0.464	0.560	0.641	0.719
6	0.079	0.163	0.265	0.355	0.448	0.547	0.630	0.712
7	0.078	0.169	0.249	0.310	0.398	0.449	0.513	0.563
8*	0.012	0.022	0.040	0.056	0.071	0.084	0.089	0.110
				Radial Displacement (mils)				
0*	-0.012	-0.019	0.010	0.026	0.001	0.002	-0.009	-0.028
1	0.002	0.004	0.010	0.029	0.048	0.052	0.072	0.090
2	-0.002	-0.005	0.006	0.034	0.049	0.060	0.079	0.106
3	0.003	0.016	0.028	0.037	0.067	0.101	0.131	0.166
4	-0.004	0.004	0.032	0.057	0.102	0.133	0.151	0.183
5	0.005	0.020	0.048	0.079	0.112	0.140	0.164	0.195
6	0.015	0.009	0.027	0.059	0.075	0.111	0.135	0.158
7	0.027	0.030	0.028	0.028	0.036	0.051	0.062	0.084
8*	-0.000	-0.001	-0.001	-0.002	0.004	0.004	0.003	0.003
Loading Rate (pounds/sec)	2700	4200	5200	5800	5800	5800	4800	3900
Rod Displacement (mils)	0.344	0.672	0.921	1.155	1.373	1.607	1.803	2.025

*Displacement shown for z = 0 and 8 in. is the displacement for the top loading plate and triaxial cell base respectively.

Table A-24: Test Data for σ_r = 10 psi, N = 2.51 millions, and Slow Loading Rate

Test 24

	LOAD (POUNDS)							
	100	200	300	400	500	600	700	800
z (in)	Vertical Displacement (mils)							
0*	0.238	0.571	0.898	1.180	1.450	1.681	1.905	2.063
1	0.196	0.425	0.634	0.850	1.033	1.219	1.381	1.513
2	0.162	0.383	0.581	0.776	0.949	1.109	1.244	1.356
3	0.169	0.367	0.547	0.729	0.881	1.033	1.158	1.263
4	0.140	0.321	0.486	0.637	0.792	0.917	1.022	1.124
5	0.149	0.296	0.469	0.655	0.785	0.912	1.030	1.144
6	0.137	0.309	0.480	0.672	0.803	0.955	1.061	1.176
7	0.144	0.305	0.444	0.596	0.716	0.831	0.906	0.963
8*	0.007	0.015	0.029	0.047	0.061	0.069	0.082	0.097
	Radial Displacement (mils)							
0*	0.006	0.008	0.020	0.019	0.009	0.017	0.011	0.002
1	0.002	0.016	0.029	0.062	0.082	0.088	0.125	0.145
2	0.009	0.045	0.069	0.110	0.137	0.172	0.225	0.250
3	0.013	0.055	0.091	0.166	0.251	0.307	0.350	0.409
4	0.020	0.067	0.106	0.172	0.248	0.321	0.380	0.434
5	0.011	0.074	0.117	0.170	0.265	0.316	0.364	0.414
6	0.007	0.037	0.071	0.120	0.180	0.220	0.265	0.303
7	-0.006	-0.013	-0.002	0.029	0.052	0.077	0.097	0.117
8*	-0.000	-0.000	-0.001	-0.001	-0.002	-0.002	-0.002	-0.003
Loading Rate (pounds/sec)	2800	4600	5600	6100	6100	5900	5500	4400
Rod Displacement (mils)	0.453	0.901	1.297	1.664	1.963	2.239	2.504	2.741

*Displacement shown for z = 0 and 8 in. is the displacement for the top loading plate and triaxial cell base respectively.

Appendix B
Stress-Strain Data

This appendix contains eight tables of stress-strain data used for analysis. Each table represents three tests. Each test was made at one of three levels of confining pressure, at either the fast or the slow loading rate, and at one of four levels of accumulated load applications, N.

These data were obtained directly from the tables given in Appendix A by the methods described in Section 4, and were plotted on Figures 4 through 7.

Table B-1: Test Data for N = 0.05 million and Fast Loading Rate

TEST NUMBER	N 10^6 Cycles	σ_r psi	σ_z psi	ε_z mils/in	ε_θ mils/in	$\frac{\partial\sigma_z}{\partial t}$ psi/sec
1	0.04	10	13.54	0.017	0.046	410
			17.07	0.086	0.155	520
			20.60	0.168	0.322	530
			24.10	0.228	0.484	540
			27.70	0.280	0.618	550
			31.20	0.319	0.723	520
			34.80	0.355	0.810	450
			38.30	0.381	0.876	300
2	0.05	20	23.54	0.020	0.020	500
			27.07	0.050	0.056	620
			30.60	0.083	0.116	710
			34.10	0.125	0.189	690
			37.70	0.172	0.272	610
			41.20	0.212	0.353	570
			44.80	0.250	0.423	490
			45.30	0.279	0.483	320
3	0.05	30	33.54	0.014	0.010	480
			37.07	0.032	0.028	730
			40.60	0.052	0.051	810
			44.10	0.079	0.079	800
			47.70	0.106	0.114	740
			51.20	0.135	0.155	660
			54.80	0.161	0.197	530
			58.30	0.184	0.236	330

Table B-2: Test Data for N = 0.06 million and Slow Loading Rate

TEST NUMBER	N 10^6 Cycles	σ_r psi	σ_z psi	ε_z mils/in	ε_θ mils/in	$\frac{\partial \sigma_z}{\partial t}$ psi/sec
4	0.06	10	13.54	0.032	0.031	100
			17.07	0.090	0.120	120
			20.60	0.159	0.268	130
			24.10	0.224	0.408	160
			27.70	0.268	0.511	160
			31.20	0.308	0.592	170
			34.80	0.334	0.653	180
			38.30	0.360	0.704	180
5	0.06	20	23.54	0.019	0.015	100
			27.07	0.052	0.050	140
			30.60	0.085	0.097	150
			34.10	0.126	0.161	160
			37.70	0.169	0.234	170
			41.20	0.209	0.305	160
			44.80	0.247	0.372	160
			48.30	0.274	0.420	150
6	0.06	30	33.54	0.015	0.010	100
			37.70	0.037	0.025	150
			40.60	0.059	0.046	160
			44.10	0.078	0.073	180
			47.70	0.103	0.104	170
			51.20	0.133	0.142	160
			54.80	0.161	0.180	160
			58.30	0.185	0.215	160

Table B-3: Test Data for N = 0.24 million and Fast Loading Rate

TEST NUMBER	N 10^6 Cycles	σ_r psi	σ_z psi	ε_z mils/in	ε_θ mils/in	$\frac{\partial\sigma_z}{\partial t}$ psi/sec
7	0.24	30	33.54	0.010	0.007	400
			37.70	0.026	0.018	500
			40.60	0.041	0.037	600
			44.10	0.055	0.060	590
			47.70	0.073	0.088	550
			51.20	0.094	0.117	450
			54.80	0.112	0.146	360
			58.30	0.130	0.178	180
8	0.24	20	23.54	0.015	0.013	370
			27.07	0.034	0.038	510
			30.60	0.057	0.073	550
			34.10	0.086	0.119	550
			37.70	0.113	0.172	480
			41.20	0.138	0.222	440
			44.80	0.160	0.267	340
			48.30	0.176	0.310	170
9	0.24	10	13.54	0.026	0.020	370
			17.07	0.064	0.079	460
			20.60	0.101	0.166	500
			24.10	0.137	0.256	520
			27.70	0.173	0.338	480
			31.20	0.197	0.405	430
			34.80	0.215	0.457	330
			38.30	0.233	0.505	170

Table B-4: Test Data for N = 0.29 million and Slow Loading Rate

TEST NUMBER	N 10^6 Cycles	σ_r psi	σ_z psi	ε_z mils/in	ε_θ mils/in	$\frac{\partial \sigma_z}{\partial t}$ psi/sec
10	0.29	30	33.54	0.010	0.010	100
			37.07	0.027	0.016	150
			40.60	0.051	0.040	200
			44.10	0.070	0.064	230
			47.70	0.098	0.100	240
			51.20	0.121	0.135	250
			54.80	0.144	0.177	240
			58.30	0.172	0.216	250
11	0.29	20	23.54	0.020	0.009	100
			27.07	0.046	0.037	160
			30.60	0.075	0.076	210
			34.10	0.113	0.132	220
			37.70	0.144	0.192	230
			41.20	0.185	0.259	240
			44.80	0.210	0.310	230
			48.30	0.242	0.359	220
12	0.29	10	13.54	0.038	0.025	100
			17.07	0.086	0.078	150
			20.60	0.135	0.164	200
			24.10	0.178	0.251	230
			27.70	0.214	0.331	230
			31.20	0.246	0.391	250
			34.80	0.278	0.443	240
			38.30	0.303	0.484	230

Table B-5: Test Data for N = 0.73 million and Fast Loading Rate

TEST NUMBER	N 10^6 Cycles	σ_r psi	σ_z psi	ε_z mils/in	ε_θ mils/in	$\frac{\partial \sigma_z}{\partial t}$ psi/sec
13	0.73	10	13.54	0.016	0.010	320
			17.07	0.045	0.032	500
			20.60	0.074	0.070	610
			24.10	0.100	0.108	660
			27.70	0.122	0.148	660
			31.20	0.143	0.182	620
			34.80	0.162	0.209	540
			38.30	0.179	0.233	420
14	0.73	20	23.54	0.013	0.004	330
			27.07	0.027	0.015	570
			30.60	0.041	0.026	650
			34.10	0.059	0.042	720
			37.70	0.076	0.063	700
			41.20	0.099	0.084	660
			44.80	0.110	0.104	580
			48.30	0.121	0.121	460
15	0.73	30	33.54	0.0122	0.0054	340
			37.07	0.0280	0.0127	520
			40.60	0.0405	0.0198	670
			44.10	0.0517	0.0276	750
			47.70	0.0629	0.0379	760
			51.20	0.0745	0.0490	690
			54.80	0.0840	0.0601	600
			58.30	0.0958	0.0742	450

Table B-6: Test Data for N = 0.80 million

and Slow Loading Rate

TEST NUMBER	N 10^6 Cycles	σ_r psi	σ_z psi	ε_z mils/in	ε_θ mils/in	$\frac{\partial \sigma_z}{\partial t}$ psi/sec
16	0.80	10	13.54	0.015	0.001	70
			17.07	0.040	0.031	130
			20.60	0.062	0.064	170
			24.10	0.084	0.100	200
			27.70	0.103	0.137	200
			31.20	0.117	0.169	210
			34.80	0.128	0.195	220
			38.30	0.142	0.212	210
17	0.81	20	23.54	0.006	0.005	80
			27.07	0.019	0.016	130
			30.60	0.030	0.026	170
			34.10	0.044	0.040	200
			37.70	0.059	0.058	210
			41.20	0.075	0.078	210
			44.80	0.089	0.096	210
			48.30	0.101	0.116	200
18	0.81	30	33.54	0.0050	0.0081	70
			37.07	0.0192	0.0139	120
			40.60	0.0283	0.0213	170
			44.10	0.0393	0.0253	200
			47.70	0.0510	0.0348	210
			51.20	0.0626	0.0429	210
			54.80	0.0733	0.0553	210
			58.30	0.0855	0.0649	200

Table B-7: Test Data for N = 2.49 million and Fast Loading Rate

TEST NUMBER	N 10^6 Cycles	σ_r psi	σ_z psi	ε_z mils/in	ε_θ mils/in	$\frac{\partial \sigma_z}{\partial t}$ psi/sec
19	2.49	30	33.54	0.0090	0.00133	360
			37.07	0.0164	0.00400	500
			40.60	0.0269	0.00822	620
			44.10	0.0365	0.01287	670
			47.70	0.0425	0.01876	650
			51.20	0.0489	0.02656	560
			54.80	0.0545	0.0343	450
			58.30	0.0607	0.0364	220
20	2.49	20	23.54	0.0054	0.0033	360
			27.07	0.0138	0.0074	530
			30.60	0.0242	0.0174	670
			34.10	0.0354	0.0301	710
			37.70	0.0449	0.0400	680
			41.20	0.0535	0.0472	630
			44.80	0.0597	0.0534	460
			48.30	0.0652	0.0594	270
21	2.49	10	13.54	0.0107	0.004	340
			17.07	0.0211	0.022	530
			20.60	0.0360	0.041	650
			24.10	0.0525	0.060	680
			27.70	0.0649	0.081	660
			31.20	0.0775	0.104	630
			34.80	0.0884	0.121	530
			38.30	0.0927	0.136	300

Table B-8: Test Data for N = 2.50 million

and Slow Loading Rate

TEST NUMBER	N 10^6 Cycles	σ_r psi	σ_z psi	ε_z mils/in	ε_θ mils/in	$\frac{\partial \sigma_z}{\partial t}$ psi/sec
22	2.50	30	33.54	0.0059	0.0042	100
			37.70	0.0130	0.0049	160
			40.60	0.0196	0.0072	200
			44.10	0.0332	0.0140	220
			47.70	0.0382	0.0220	210
			51.20	0.0392	0.0257	200
			54.80	0.0479	0.0309	170
			58.30	0.0547	0.0363	150
23	2.50	20	23.54	0.0039	0.0004	100
			27.07	0.0132	0.0044	150
			30.60	0.0204	0.0120	210
			34.10	0.0307	0.0192	210
			37.70	0.0387	0.0312	210
			41.20	0.0474	0.0416	210
			44.80	0.0555	0.0496	170
			48.30	0.0628	0.0604	140
24	2.50	10	13.54	0.0080	0.0049	100
			17.07	0.0207	0.0218	160
			20.60	0.0304	0.0349	200
			24.10	0.0373	0.0564	220
			27.70	0.0478	0.0849	220
			31.20	0.0568	0.1049	210
			34.80	0.0685	0.1216	200
			38.30	0.0760	0.1397	160